NASA/TM—2001-211107

Low Emissions RQL Flametube Combustor Test Results

Clarence T. Chang and James D. Holdeman
Glenn Research Center, Cleveland, Ohio

July 2001

The NASA STI Program Office . . . in Profile

Since its founding, NASA has been dedicated to the advancement of aeronautics and space science. The NASA Scientific and Technical Information (STI) Program Office plays a key part in helping NASA maintain this important role.

The NASA STI Program Office is operated by Langley Research Center, the Lead Center for NASA's scientific and technical information. The NASA STI Program Office provides access to the NASA STI Database, the largest collection of aeronautical and space science STI in the world. The Program Office is also NASA's institutional mechanism for disseminating the results of its research and development activities. These results are published by NASA in the NASA STI Report Series, which includes the following report types:

- TECHNICAL PUBLICATION. Reports of completed research or a major significant phase of research that present the results of NASA programs and include extensive data or theoretical analysis. Includes compilations of significant scientific and technical data and information deemed to be of continuing reference value. NASA's counterpart of peer-reviewed formal professional papers but has less stringent limitations on manuscript length and extent of graphic presentations.

- TECHNICAL MEMORANDUM. Scientific and technical findings that are preliminary or of specialized interest, e.g., quick release reports, working papers, and bibliographies that contain minimal annotation. Does not contain extensive analysis.

- CONTRACTOR REPORT. Scientific and technical findings by NASA-sponsored contractors and grantees.

- CONFERENCE PUBLICATION. Collected papers from scientific and technical conferences, symposia, seminars, or other meetings sponsored or cosponsored by NASA.

- SPECIAL PUBLICATION. Scientific, technical, or historical information from NASA programs, projects, and missions, often concerned with subjects having substantial public interest.

- TECHNICAL TRANSLATION. English-language translations of foreign scientific and technical material pertinent to NASA's mission.

Specialized services that complement the STI Program Office's diverse offerings include creating custom thesauri, building customized data bases, organizing and publishing research results . . . even providing videos.

For more information about the NASA STI Program Office, see the following:

- Access the NASA STI Program Home Page at ***http://www.sti.nasa.gov***

- E-mail your question via the Internet to help@sti.nasa.gov

- Fax your question to the NASA Access Help Desk at 301–621–0134

- Telephone the NASA Access Help Desk at 301–621–0390

- Write to:
  NASA Access Help Desk
  NASA Center for AeroSpace Information
  7121 Standard Drive
  Hanover, MD 21076

NASA/TM—2001-211107

Low Emissions RQL Flametube Combustor Test Results

Clarence T. Chang and James D. Holdeman
Glenn Research Center, Cleveland, Ohio

National Aeronautics and
Space Administration

Glenn Research Center

July 2001

Acknowledgments

Those who were particularly responsible for elements of the test program were: Daniel C. Briehl, Valerie J. Lyons, C. Joe Morgan, H. Lee Nguyen, Richard W. Niedzwiecki, and Robert R. Tacina. The original manuscript was prepared by H. Lee Nguyen; this version was assembled and edited by Clarence T. Chang and James D. Holdeman.

Document Availability Change Notice

This document was published in July 2001 with an EAR restriction.
It was changed April 2003 to Unclassified/Unlimited per DAA modified February 11, 2003.

Per the STI Program Office and Code I at Headquarters,
you may modify copies in your possession. The restriction notice
on the cover, title page, and report documentation page, should be
boldly crossed out and the above statement printed clearly above or below it.

Available from

NASA Center for Aerospace Information
7121 Standard Drive
Hanover, MD 21076

National Technical Information Service
5285 Port Royal Road
Springfield, VA 22100

Available electronically at http://gltrs.grc.nasa.gov

TABLE OF CONTENTS

LIST OF TABLES

LIST OF FIGURES

NOMENCLATURE

A_m	mainstream flow area, in^2
ACd	quick-mix injection effective discharge area, in^2
CO	carbon monoxide
CO_2	carbon dioxide
$EI(NO_x)$	NO_x emission index, g/(kg-fuel), assuming all emissions are NO_2
EI(CO)	CO emission index, g/(kg-fuel)
EI(UHC)	unburnt hydrocarbon emission index, g/(kg-fuel)
F/A_m	overall fuel-to-air ratio, from metered flow
F/A_s	overall fuel-to-air ratio, from gas sample
F/A_{stoich}	stoichiometric fuel-to-air mass ratio, 0.068
FARR	$(F/A_s) / (F/A_m)$
J	quick-mix jet to mainstream momentum-flux ratio $J = [(W_q/W_{rb})^2(T_3/T_{rb})] / [(ACd/A_m)^2(M_3/M_{rb})]$
M_3	inlet air molecular weight, g/mole
M_{rb}	rich-burn zone mean molecular weight, g/mole
NO	nitric oxide
NO_2	nitrogen dioxide
NO_x	nitrogen oxides (NO + NO_2)
O_2	oxygen
P_3	combustor inlet plenum pressure, psia
P_4	lean-burn section exit pressure, psia
P_{rb}	rich-burn section exit pressure, psia
ΔP_{34}	pressure drop from rich-burn zone inlet to lean-burn zone exit, psi
Rdg	test cell data series identification number
T_3	combustor inlet total temperature, °F
T_4	estimated lean-burn section equilibrium temperature, °F
T_{rb}	estimated rich-burn section equilibrium temperature, °F
UHC	unburnt hydrocarbon
$V_{ref,lb}$	lean-burn zone (cold flow) reference velocity, ft/s
$V_{ref,ov}$	overall (non-reacting flow) reference velocity, ft/s
$V_{ref,q}$	quick-mix zone (non-reacting flow) reference velocity, ft/s
$V_{ref,rb}$	rich-burn zone (non-reacting flow) reference velocity, ft/s
W_d	rich-burn zone dome airblast mass-flow rate, lbm/s, both fuel nozzles
W_f	fuel-flow rate, lbm/s
W_{fi}	inner fuel-flow rate, lbm/s (Textron nozzle only)
W_{fo}	outer fuel-flow rate, lbm/s (Textron nozzle only)
W_i	rich-burn zone inner airblast mass-flow rate, lbm/s, both fuel nozzles
W_m	rich-burn zone middle airblast mass-flow rate, lbm/s, Textron nozzle only
W_o	rich-burn zone outer airblast mass-flow rate, lbm/s, both fuel nozzles
W_q	quick-mix air mass-flow rate, lbm/s
W_{rba}	rich-burn zone total air mass flow rate, $W_i+W_m+W_o+W_d$, lbm/s
W_{rb}	rich-burn zone total mass flow rate, $W_{rba}+W_f$, lbm/s
η	combustion efficiency
ϕ_{lb}	lean-burn zone equivalence ratio, $(F/A_m)/(F/A_{stoch})$
ϕ_{rb}	rich-burn zone equivalence ratio
τ_{lb}	lean-burn zone residence time, ms
τ_{ov}	overall residence time, ms
τ_q	quick-mix zone residence time, ms
τ_{rb}	rich-burn zone residence time, ms

1. Introduction

The overall objective of this test program was to demonstrate and evaluate the capability of the Rich-burn/Quick-mix/Lean-burn (RQL) combustor concept for HSR applications. This test program was in support of the Pratt & Whitney and GE Aircraft Engines HSR low-NO_x Combustor Program. Collaborative programs with Parker Hannifin Corporation and Textron Fuel Systems resulted in the development and testing of the high-flow low-NO_x rich-burn zone fuel-to-air ratio research fuel nozzles used in this test program.

The specific objectives of this test program were to:

1) Demonstrate the capability of the RQL staged combustor to reach the program goal of low NO_x emissions at supersonic cruise conditions.

2) Obtain test data to help validate and develop analytical models that may be used to design improved low emissions combustors (Staff, *Lewis News*, 1991).

2. Test Combustor

The test rig was mounted in stand 1 of the CE-5B test facility in the Engine Research Building at the NASA Lewis Research Center. The facility could supply the combustor inlet with pressurized air of 16 atm at 1100 °F by means of a non-vitiating heat exchanger. Combustion gases were sampled continuously during testing. Three water-cooled sampling probes were located at the axial stations shown in figure 1; 6 in. (probe A), 12 in. (probe B), and 25 in. (probe C) downstream of the lean burner inlet. Gas sampling probes A and B were 5-point probe designs and they took ganged-samples from locations 0, 1.565, 2.213, 2.711, and 3.130 in. from the centerline of the lean burner. Gas sampling probe C was a 10-point probe design and it took ganged-sample measurements from locations 0, 0.572, 1.025, 1.583, 2.393, 4.607, 5.417, 5.975, 6.428, and 6.82 in.across the lean-burn zone diameter.

[Editor's note: The original 1992 draft did not specify whether the reported emissions values were wet or dried. However, the author of that report indicated that the samples were dried before measurements were taken. All of the data reported here (except the smoke numbers in Table 5) are corrected wet readings.]

The cylindrical flame tube rig dimensions are given in figure 1. Hot ceramic liners were used to minimize the effects of heat loss on NO_x emissions. Figure 2 shows a schematic diagram of the RQL combustor facility. All of the air was divided between the rich zone and the mixer; there was no air addition in the lean zone.

The quick-mix configuration used in all the tests for which results are reported herein was a single row of eight 45° slanted slots; each was 1.99 in. long and 0.33 in. wide. Liquid fuel, JP-5, at ambient temperature was injected into the combustor rig using either the Parker Hannifin Airblast Low NO_x Nozzle (Phase I) or a Textron Turbo Component Airblast Fuel Nozzle. [Ed: Herein referred to as "Parker" and "Textron" fuel nozzles.]

A cross-section of the Parker fuel nozzle is shown in figure 3. This airblast fuel nozzle was assembled with co-swirling 60° helical air swirlers for the dome air (W_d), the outer airblast air (W_o), and the inner airblast air (W_i). A 60° straight cut was made for the co-swirling fuel swirler. The fuel nozzle's three air circuits were controlled and metered separately. The mixer section had

the slots angled to reinforce the fuel nozzle swirl. The effective discharge areas are in Table 1.

The cross-section of the Textron fuel nozzle is shown in figure 4. This dual airblast fuel nozzle was assembled with co-swirling 60° helical air swirlers for the dome air, the outer air, the middle air, and the inner air circuit. There were two 60° co-swirling fuel swirlers for the outer and inner fuel passages and a 60° counter-swirling helical air swirler for the inner air circuit. The dome air (W_d), the outer (W_o), the middle air (W_m), and inner air (W_i), were controlled and metered separately. The outer and inner fuel flow split (W_{fo} and W_{fi}) could also be varied. All the air and fuel streams in the fuel nozzle swirl in the same direction; the quick-mixing section had swirl slots angled to oppose the fuel nozzle swirl. The effective discharge areas are in Table 1. Note that data obtained prior to 91/7/30 are not reported herein.

[Ed.: It appears that the outer and the middle air circuits shared a common metering circuit and were never operated separately. Secondly, there appeared to be no provision in the test facility to control the fuel split between the inner and the outer fuel circuits, even though the designed split was for 60% of the fuel to flow through the outer circuit. Thus, the flow split was apparently assumed by the original author. A test on a second date had the outer passage sealed so that all of the fuel flowed through the iner passage.]

3. Combustor Test Results

Prior to combustion testing, flow tests were performed to calibrate the discharge orifices. The effective flow discharge areas are tabulated in Table 1 along with the experiment dates and record numbers. Figure 5 compares the measured discharge pressure drops versus those calculated from metered flow rates.

3.1 Parker Fuel Nozzle Tests

An investigation was conducted of the effect of various parameters of the Parker fuel nozzle on NO_x emissions and combustor performance. The results are listed in Table 2 and are shown in figures 6 to 8. Data in these figures were obtained with probes A, B, and C respectively. Parts (a) to (d) of each figure are NO_x, CO, CO_2, and combustion efficiency (η). These results were obtained by altering the Parker fuel nozzle's individual air circuit flow rates (i.e. W_o, and W_i) for a fixed fuel nozzle air flow (W_{rba}) and fixed combustor operating conditions.

A 5-in. ID quick-mix section was used in this test. [Ed.: The application of a 5-in. ID quick-mix section does not correlate with the J values listed in the author's original draft. A 4-in. ID unit fits very well, however. We suspect that there were 8 45° slanted slots, but the physical size of each of the slots is unknown]

The prioritized influence from the three fuel nozzle air circuits on the reduction of EI(NO_x) can be sequenced as W_i, W_o, and W_d. This suggests that for the Parker fuel nozzle, the inner and outer air velocities and volume flow rates have more dominant effects on spray atomization and fuel spatial distribution than does the dome air.

Bench tests conducted at Parker Hannifin showed that increasing the inner air and outer air flows were more effective in decreasing drop size SMD than the dome air (Sun & Nguyen, 1992). This SMD result is consistent with the NO_x emissions measurements. Drop sizes SMD decrease as the inner air and outer air pressure drops increase. This effect of inner and outer air pressure drop on SMD levels off at the same inner and outer air pressure drop values.

Figures 6a, 7a, and 8a suggest that the lower W_d/W_{rba} condition gave lower NO_x emissions than the higher W_d/W_{rba} conditions. This is consistent with the improved atomization due to more air diverted for atomization.

The CO emissions results displayed almost the same trend as the NO_x emissions results (see figures 6b, 7b, and 8b). The CO_2 and combustion efficiency results also display the same trend. The low EI(NO_x), low EI(CO), high CO_2, and high combustion efficiency also suggest the effect of fuel-air mixing, local fuel-air ratio, and recirculation in the rich burner tested.

The Parker fuel nozzle sensitivity study showed a significant but decreasing difference between the maximum and minimum EI(NO_x) measured for data obtained with gas sampling probes A, B, and C. The observed difference for gas sampling probe A data were due to the effect of the rich burner, and possibly quick mixer and rich burner/quick mixer interaction. The smaller differences observed for gas sampling probes B and C data are due to the off-setting effect of longer lean burner residence time.

3.2 Textron Fuel Nozzle Tests

The nominal design air flow splits of the Textron fuel nozzle were 47.6%, 25.5%, 19.1%, and 7.7% of the total fuel nozzle air flow rate for the dome, outer air, middle air, and inner air circuits respectively. Bench tests performed at Textron Fuel Systems showed high levels of atomization achieved (~10 μm SMD) at the above air flow splits for selected air-fuel ratios (F. Phil Lee private communication). During combustion tests, the dome air (W_d), the outer air (W_o) plus the middle air (W_m), and the inner air (W_i) were separately controlled and metered.

Figures 9 to 11 show results of investigating the effect of the Textron fuel nozzle on NO_x emissions and combustor performance. The corresponding flow variables are listed in Table 3. These results were obtained by altering the Textron fuel nozzle individual air circuit flow rates and the inner and outer fuel flow rates (W_{fi} and W_{fo}). Tests were conducted at target conditions of 800 °F T_3, 120 psia rig exhaust pressure (P_4), 0.024 metered overall fuel-air ratio (F/A_m), 2.0 rich burner equivalence ratio (ϕ_{rb}), and 1.63 lbm/s rich burner air flow (W_{rba}).

A few of the data points were obtained at T_3 of 840 °F, W_{rba} of 1.83 lbm/s, with the ratio $(W_o+W_m)/W_i$ of 1.5 and with W_d/W_{rba} of 47.6%, 39.5%, and 35.2%, respectively (as shown in figure 9 to 11). Two levels of W_{fo}/W_{fi} =1.5 and 0 were investigated. A 4-in. ID quick-mix section with eight 45° slanted slots with each slot having a length of 1.99 in. and a width of 0.33 in. was used.

For the Textron fuel nozzle, smaller differences in NO_x emissions levels were observed for $(W_o+W_m)/W_i$ above 3.8 for all conditions (see Figs. 9a, 10a, and 11a). Variation of Parker individual air circuit flow rates showed bigger differences in EI(NO_x) measured between conditions tested (See Figs. 6a, 7a, and 8a).

For this fuel nozzle, the difference between the maximum and minimum EI(NO_x) for gas sampling probes A, B, and C data monotonically decreased. This suggested the fuel nozzle effect may have been offset by the effect of longer lean burner residence time (τ_{lb}). The differences between the highest and lowest EI(NO_x) are smaller for the Textron fuel nozzle than the Parker fuel nozzle.

Also, the minimum EI(NO_x) was obtained with the Textron fuel nozzle operated near the nominal design point of the fuel nozzle. For the Textron fuel nozzle, the 47.6% W_d/W_{rba}, 17.9% W_o/W_{rba}, 13.5% W_m/W_{rba}, 21% W_i/W_{rba} and with W_{fo}/W_{fi} =1.5 gave the same EI(NO_x) value as the Parker fuel nozzle with 22% W_d/W_{rba}, 39% W_o/W_{rba}, and 39% W_i/W_{rba} at the similar combustor operating condition. For cases investigated with the Textron fuel nozzle, the 47.6% W_d/W_{rba}, with equal splits of the remaining fuel nozzle air to W_o, W_m, and W_i and with W_{fo}/W_{fi} =1.5 gave optimal EI(NO_x) at low fuel nozzle pressure loss.

The case with W_{fo}/W_{fi} =0 and with 23.8% W_d/W_{rba}, with equal splits of the remaining fuel nozzle air to W_o, W_m, and W_i gave low EI(NO_x) together with lowest EI(CO) at reasonable fuel nozzle pressure loss. In this case, the high pressure loss through the W_i counter-swirl circuit gave a spray angle of 80° at design point, enhanced fuel-air interaction, recirculation and atomization.

3.3 Combustor Parametric Study Using Parker Fuel Nozzle

A parametric study was conducted to investigate the effect of combustor operating variables on EI(NO_x) and combustor performance. For these tests, the Parker fuel nozzle setting was 22% W_d/W_{rba}, with 39% of the fuel nozzle air for W_o and W_i each. A 4 in. ID quick-mix section was used with eight 45° slanted slots with each slot having a length of 1.9 in. and a width of 0.33 in.

Combustor parametric tests were conducted at inlet temperatures (T_3) from 600 to 1100 °F, rig rich-burn pressure (P_{rb}) of 80 to 150 psia, exit temperatures (T_4) of 2600 to 2900 °F with a few test points at 3160 °F, overall reference velocities ($V_{ref,ov}$) of 50 to 150 ft/s, and rich-burn equivalence ratio (ϕ_{rb}) of 1.5 to 2.2. These data are given in Table 4 and are shown in figures 12 to 19.

[Ed: The *J* values in Table 4 were calculated using the formula in the Nomenclature, assuming a *Cd* of 0.73 for the quick-mix jets. These *J* values are within 8% of those reported in the original internal report.]

3.3.1 Lean Burner Exit Temperature Parametric Study

NO_x and CO results from tests with variation in lean burner adiabatic temperature are shown in figures 12 and 13, respectively. These conditions were achieved by decreasing the quick-mix air flow rate (W_q) at constant rich-burn air flow rate (W_{rba}) and fuel flow rate (W_f) with ϕ_{rb} of 2.0 and other fixed combustor operating conditions. Therefore, increasing lean burner adiabatic temperature (T_4), or overall equivalence ratio (ϕ_{ov}) also decreased the mixer momentum-flux ratio (J), and slightly decreased $V_{ref,ov}$ over the range of T_4. Increasing T_4 increased the EI(NO_x) slightly. Figures 12a & 12b show variation of EI(NO_x) with T_4 at constant P_{rb}, T_3, and $V_{ref,ov}$. These constant P_{rb}, T_3, $V_{ref,ov}$ curves have the same slope over the range of T_4 tested (nominally 2600 to 2900 °F with a few data points at 3160 °F) observed within the probe A and probe B data.

Increasing T_4 from 2600 to 2900 °F reduces J by almost half. The reduction in J would be expected to reduce quick-mix jet penetration. A degradation in quick mixing efficiency could cause an additional increase in EI(NO_x) measured. Novick and Troth (1981) and Pierce et al. (1980) reported little or no effect of ϕ_{lb} on EI(NO_x) for ERBS fuel and No. 2 diesel fuel.

Carbon monoxide (CO) emissions, on the other hand, were influenced significantly by T_4. The higher T_4 increased the CO reaction rate and resulted in lower CO emissions (see Figs. 13a & 13b).

All the CO levels measured were below an EI(CO) level of 10 and are similar to the equilibrium CO levels except at 600 °F T_3. The high levels of CO measured at 600 °F T_3 at gas sample probe A were due to low T_3, low T_4, short residence times, and high J. The CO levels measured with gas sample probe B (Fig. 13b) were very low (below EI level of 2; except for T_3 of 600 °F the EI(CO) levels are between 2 to 10).

3.3.2 Combustor Inlet Temperature (T_3) Parametric Study

Results from tests with variation in T_3 are shown in figures 14 and 15. These conditions were achieved by varying T_3 at constant T_4, at a ϕ_{rb} of 2 and at nominally constant V_{ref} in each of the three zones. W_{rba} and W_q were adjusted. Therefore, during these tests, increasing T_3 also increases T_{rb}. If either W_q/W_{rb} or T_3/T_{rb} increased, so did J.

Increasing T_3 increased NO_x emissions considerably as shown in figure 14. This figure shows variation of EI(NO_x) over a range of T_3 of 600 to 1100 °F and at constant P_{rb} and $V_{ref,ov}$. Figures 12a & 12b suggest that curves with different T_3's have similiar variations with T_4. Similar trends with T_3 can be observed in figures 14a, 14c, and 14e. This indicates that a similar T_4 effect was observed for higher T_3 levels, and also that a similar T_3 effect was observed for the measured T_4 levels.

The significant effect of T_3 on EI(NO_x) was also reported by Novick and Troth (1981) and Pierce et al. (1980) for natural gas, and No. 2 fuel oil. Melconian (private communication) also observed a significant effect of T_3 (more dominant than the T_4 effect) on EI(NO_x) in a recent engine test program running the Variable Residence Time combustor in a fuel rich - quick mix - fuel lean mode.

Increasing T_3 increases reaction rates, hence thermal NO_x reaction and CO reaction rates increase with T_3. Comparing curves between figures 14a & 14b, 14c & 14d, and 14e & 14f show the same slope. This suggests that lean burner residence time displays a similar effect on NO_x reactions rates for these T_3 levels.

During these tests, increasing T_3 also increased T_{rb}. The higher T_{rb} would increase rich zone NO_x levels if there were local uneven distributions of fuel in the rich burner (F/A_{rb}). During these tests, the higher J is due to an increase in T_3 (especially at 1100 °F), and at low T_4, e.g. 2600 °F. This might cause jet overpenetration and result in poorer mixing. However, higher T_3 increases fuel spray vaporization rate and atomization (due to a decrease in fluid viscosity). This rich burner effect is offset by the other adverse effect (on NO_x) mentioned above.

The dominant effect of higher T_3 on increasing the CO reaction rate resulted in lower CO emissions as shown in figure 15. All EI(CO) measured are low (<10) except for data with T_3 of 600 °F obtained with gas sample probe A.

3.3.3 Combustor Pressure Parametric Study

NO_x and CO results from tests with variation in combustor pressure are shown in figures 16 and 17. These conditions were achieved by varying the combustor pressure [Ed.: We think this is P_{rb}.] over a range of 80 to 150 psia at constant T_3, T_4, J, V_{ref} in the three zones, with ϕ_{rb} of 2 (i.e. at constant T_{rb}). Therefore increasing P_{rb} also increased W_{rba}, and W_q. Increasing P_{rb} increased NO_x emissions. Similar pressure effects on NO_x were reported by Rizk and Mongia (1990 &

1991) for ERBS, No. 2 fuel, and RESID fuel. Pierce et al. (1980) also reported a pressure effect on NO_x for No. 2 fuel.

The observed presure effect suggested the sensitivity of rich burner (fuel preparation and rich burner residence time (τ_{rb})) and the mixing section and possibly rich burner/quick mixer interaction on NO_x levels. Increasing P_{rb} would decrease the spray cone angle.

Rizk and Mongia (1990 & 1991) also reported that the effect of increasing the system pressure was to increase the initial NO formed in the dome region of the rich burner for the case where there is poor local fuel-air distribution in this region. They also reported that the rate of NO reduction at higher pressures is more significant than at lower pressure level and that no pressure effect is noticed at large rich burner residence time.

Comparing curves between figures 16e and 16f shows that data obtained with gas sample probe B have smaller slopes than data obtained with gas sample probe A. This trend is also observed in the dependency of NO_x on combustor pressure and lean burner residence time (τ_{lb}) from the NO_x correlation equations to be described later.

In the quick-mix section, increasing pressure increases the dissociation of oxygen molecules, increases the flame thickness, stretches out the flame zones and increases the number of turbulent eddies with hot surface areas (due to an accompanying increase in mass-flow rates in these tests which resulted in an increase in the Reynolds number). An undesirable combination of the effects mentioned above together with a slower quick-mix rate and a non-uniform rich burner exit gases profile would increase the NO_x level.

Rosfjord (1986) reported a pressure insensitivity to NO_x control with τ_{rb} at nominally 220-ms. For the same series of tests, Rosfjord also reported no influence of τ_{lb} on NO_x level for a range of τ_{rb} of 150 to 220 ms. This suggests that the long τ_{rb} may offset the pressure effect on NO_x in the rich burner.

In contrast to the pressure effect on EI(NO_x), increasing combustor presure decreases EI(CO) as shown in figure 17.

3.3.4 Combustor Overall Reference Velocity Parametric Study

Results from tests with variation in overall reference velocity ($V_{ref,ov}$) are shown in figures 18 and 19. These conditions were achieved by varying air flow rates and fuel flow rate and anchoring all other combustor variables. These tests were conducted at ϕ_{rb} of 2. Therefore during these tests, increasing $V_{ref,ov}$ also increased the rich burner and quick mixer reference velocities ($V_{ref,rb}$ and $V_{ref,q}$) and decreased the hot residence times in the rich burner, quick mixer, and lean burner sections. Higher mass flow rates might enhance the mixing rates.

Figures 18a, 18c, and 18e show the insensitivity of NO_x emissions to a variation in $V_{ref,ov}$ for the gas sample probe A data. This suggests that over the range of $V_{ref,ov}$ tested, 65 to 140 ft/s, the induced altered mixing rate and the altered residence time in the rich burner and quick mixing section tested show no infuence on NO_x emissions.

Figures 18b, 18d, and 18f indicate a small inverse relationships between $V_{ref,ov}$ and EI(NO_x). This suggests the effect of additional dynamic pressure loss between the gas sampling probes A and B locations on NO_x emissions levels obtained with the gas sampling probe B.

Novick and Troth (1981) reported that ϕ_{rb} for minimum NO_x became more fuel lean with decreasing residence time. The fuel used in these authors' test was ERBS. This point bears an impact on variable geometry controls and is worthy of consideration for future investigations.

Increasing $V_{ref,ov}$ gives a small increase in CO emissions as shown in figure 19.

3.3.5 Lean Burner Residence Time Parametric Study

The true role of lean burner residence time is clearly identified by comparing data obtained with gas sampling probes A and B in figures 12 to 19. In general, doubling the lean burner residence time only slightly increased the EI(NO_x). The CO emissions levels obtained with gas sampling probe B are much less than that obtained with gas sampling probe A.

3.3.6 Rich Burner Equivalence Ratio (ϕ_{rb}) Parametric Study

NO_x and CO results for tests with variation in ϕ_{rb} in the range of 1.5 to 2.25 are shown in figures 20 and 21. These conditions were achieved by varying the rich burner and quick-mix section air flow rates at constant fuel flow rate and total air flow rate (cf. Rdgs. 921A to 931B, 934A - 937B, 788A, 789B, 803A, and 804B listed in Table 4), while maintaining other combuster conditions constant. Therefore during these tests, increasing ϕ_{rb} also decreased T_{rb}, decreased $V_{ref,rb}$ and increased J. For example, variation of ϕ_{rb} from 1.53 to 2.24 as shown in Rdg. nos. 920A - 930B resulted in an increase in J from 7.1 to 25.5, a decrease in T_{rb} from 3430 to 2490 °F, and a decrease in $V_{ref,rb}$ from 42.5 to 28.7 ft/s. Figure 20a indicates that there is a slight increase in EI(NO_x) for a corresponding increase in ϕ_{rb} from 1.63 to 2.0 at T_3 of 600 and 840 °F.

From this limited number of tests, the results seemed to suggest that it is more beneficial to operate this RQL combustor at ϕ_{rb} for minimum NO_x at higher T_3 conditions. For the case with T_3 of 600 °F, it appears that there is no change in EI(NO_x) between ϕ_{rb} of 2.0 and 2.24. Figure 20a also seems to suggest that the NO_x "bucket" may be around ϕ_{rb} of 1.4. Novick and Troth (1981) reported a NO_x "bucket" around ϕ_{rb} of 1.4 for ERBS, ERBS doped with fractional percentage of Nitrogen, RESID, and SRC-II fuels. Pierce et al. (1980) and Rosfjord (1986) reported a NO_x "bucket" around ϕ_{rb} of 1.4 for No. 2 fuel with 0.5% Nitrogen and UCC-1, UCC-2 fuels, respectively. Pierce et al. (1980) also reported a NO_x staging capability involving fixed NO_x emissions levels and NO_x minimum point as the rich burner air flow is increased from a low value of 9.8% through an intermediate value of 13.5% to a high setting of 21.4%.

Novick and Troth (1981) also reported that the ϕ_{rb} for minimum NO_x varies with residence time and pressure drop, becoming more fuel lean with decreasing residence time or with increasing pressure drop. These authors' used ERBS and RESID fuels in the tests. In the tests using RESID fuel, the minimum NO_x level is reported to increase as pressure drop is reduced. These features bear some benefits to variable geometry controls issues that they would be noteworthy for future investigations.

Figure 21 indicates an increase in CO emissions as ϕ_{rb} is increased.

3.3.7 Quick Mixer Parametric Study

Different mixing configurations were investigated from 5/24/91 to 7/09/91 (see Table 1). The data for these configurations are not reported in this report.

A 4 in. ID section with eight 45° slanted slots was adopted. (These slots were 1.99 by 0.33 in.) The performance of this configuration on EI(NO_x) is shown in figure 22 along with HSR targets and other recently related works.

The fuel-to-air ratio obtained from gas sample versus that obtained from metering is shown in figure 23. The proximity of the data scatter to the unity FARR line suggests that the measured flow was uniform at the sample probe locations.

3.4 Summary of NO_x and CO Emissions Results

In general, the results show that T_3 is the major controlling factor in the formation of NO_x, with P_4, T_4, $V_{ref,ov}$, and τ_{ov} playing secondary roles. T_3 appears to dominate probably because the NO_x formation rates accelerate as T_3 increases. Increasing T_3 increases T_{rb} and increases the rate of NO_x production.

The secondary influence of T_4 suggests that NO_x formation is directly proportional to the amount of fuel burned since T_4 has a linear relationship with the overall fuel-to-air ratio.

The overall resident time, τ_{ov}, is linked inversely to the reference velocity, $V_{ref,ov}$, aerodynamically. Speeding up $V_{ref,ov}$ reduced τ_{ov}.

High pressure effects diminish with longer lean-burn residence time. Also, the T_4 effect on post-flame thermal NO_x becomes more dominant at gas sampling probe B location.This suggests that the T_4 dependency is increased with lean-burn residence time.

The noticeable differences suggest the complexities of the NO_x formation mechanisms in the RQL combustor tested. This suggests that for τ_{lb} corresponding to gas sampling probe B location or farther downstream, the lean-burn residence time effects have leveled off and are dominated by the post-flame NO_x formation mechanisms in these lean burner regions. To predict EI(NO_x) for the RQL combustor, a correlation expression should account for the primary effects of T_3 and the secondary effects of T_4, P_{rb}, τ_{ov}, and V_{ref}.

The results suggest T_3 and T_4 dominates CO pruduction; P_{rb} and τ_{ov} have secondary effects.

3.5 Smoke Emissions Results

A limited number of smoke samples was taken for the RQL tests. The results are given in Table 5 and figures 24 and 25. Figure 24 shows the trade-off between NO_x emissions and smoke using results of Reading numbers 759A, 760B, and 762C listed in Table 5. Figure 25 indicates that the smoke number decreases as lean-burn residence time increases.

4. Conclusions

Based on the results obtained in this test program, several conclusions can be made:

1. The RQL tests gave low NO_x and CO emissions results at conditions corresponding to HSR cruise.

2. The Textron fuel nozzle design with optimal multiple partitioning of fuel and air circuits shows potential of providing an acceptable uniform local fuel-rich region in the rich burner.

3. For the parameters studied in this test series, the tests have shown T_3 is the dominant factor in the NO_x formation for RQL combustors. As T_3 increeases from 600 °F to 1100 °F, EI(NO_x) increases approximatesly three fold.

4. Factors which apprear to have secondary influence on NO_x formation are P_4, T_4, ϕ_{rb}, $V_{ref,ov}$.

5. Low smoke numbers were measured for ϕ_{rb} of 2.0 at P_4 of 120 psia.

References

Hatch, M.S., Sowa, W.A., Samuelsen, G.S., and Holdeman, J.D. (1992). "Jet Mixing Into a Heated Cross Flow in a Cylindrical Duct: Influence of Geometry and Flow Variations," AIAA-92-0773.

Lew, H.G., Carl, D.R., Vermes, G., DeZubay, E.A. (1981). "Low NO_x Heavy Fuel Combustor Concept Program. Phase 1: Combustion Technology Generation," NASA-CR-165482, DOE/NASA/0146-1.

Novick, A.S., and Troth, D.L. (1981). "Low NO_x Heavy Fuel Combustor Concept Program," NASA CR-165367, DOE-NASA-014B-1, October, 1981.

Pierce, R.M., Mosier, S.A., and Smith, C.E. (1980). "Final Report - Advanced Combustor Systems for Stationary Gas Turbine Engines, Vol. II," Contract No. 68-02-2136, FR-11405.

Risk, N.K., and Mongia, H.C. (1990). "Ultra Low NO_x Rich Lean Combustion," ASME Paper 90-GT-87.

Risk, N.K., and Mongia, H.C. (1991). "Low NO_x Rich-Lean Combustion Concept Application," AIAA-91-1962.

Rosfjord, T. J. (1981). "Evaluation of Synthetic-Fuel-Character Effects on Rich-Lean Stationary-Gas-Turbine Combustion Systems. Volume 1: Subscale Test Program," EPRI-AP-2822-Vol-1.

Rosfjord, T.J. (1986). "Coal-Water Mixture Combustion Technology Development," Final Report DOE/MC/20404-2079.

Smith, C.E., Talpallikar, M.V., and Holdeman, J.D. (1991). "A CFD Study of Jet Mixing in Reduced Areas for Lower Combustor Emissions," AIAA-91-2060.

Staff, Lewis News (1991). "Team Spirit Pushes NO_x Emission Program Ahead," *Lewis News*, August 2.

Shultz, D.F., and Wolfbrandt, G. (1980). "Flame Tube Parametric Studies for Control of Fuel Bound Nitrogen Using Rich-Lean Two Stage Combustion," NASA-TM-81472, 1980.

Sun, F. T.-Y., and Nguyen, H. L. (1992). "Development of the NASA High Flow Low NO_x Research Nozzle," ILASS-Americas.

Tacina, R.R. (1990) "Low NO_x Potential of Gas Turbine Engines," AIAA-90-0500 / NASA-TM-102452.

Table 1: RQL combustor test record

Date yymmdd	Rdgs.	Dome *ACd* in^2	Outer *ACd** in^2	Inner *ACd* in^2	Quick-mix *ACd*† in^2	Quick-mix ID in	Mixing Configuration	Issue
910517	152-164	0.93	0.347	0.176	2.3	5	?	Flow calibration test
910524	169-180	0.93	0.347	0.176	2.3	5	?	
910524	181-207	0.93	0.347	0.176	3	5	2-rows of 24 45°-slots (0.88-by-0.221)	
910614	233-257	0.93	0.347	0.176	3.4	5	1-row of 12 45°-slots‡	
910620	258-338	0.93	0.347	0.176	3	5	2-rows of 24 holes 1.9 in. apart (0.5 in. ID)	
910627	339-380	0.93	0.347	0.176	3.3	5	2-rows of 24 holes 1.9 in. apart (0.5 in. ID)	
910709	381-510	0.93	0.347	0.176	3	5	2-rows of 24 holes 1.9 in. apart (0.5 in. ID)	
910725	512-548	0.93	0.347	0.176	3.3	5	1-row of 8 45°-slots‡	
910730	549-646	0.93	0.347	0.176	3.3	5	1 row of 8 45°-slots‡	Parker nozzle test
910801	649-694	0.93	0.347	0.176	3.3	5	1 row of 8 45°-slots‡	Parker nozzle test
911022	700-702	0.93	0.347	0.176	3.4	4	1 row of 8 45°-slots (1.99-by-0.33)	
911105	703-706	0.93	0.347	0.176	3.4	4	1 row of 8 45°-slots (1.99-by-0.33)	?
911112	707-751	0.93	0.347	0.176	3.5	4	1 row of 8 45°-slots (1.99-by-0.33)	Smoke number test
911204	756-781	0.93	0.347	0.176	3.4	4	1 row of 8 45°-slots (1.99-by-0.33)	RQL parametric test
911205	782-804	0.93	0.347	0.176	3.3	4	1 row of 8 45°-slots (1.99-by-0.33)	RQL parametric test
911211	810-887	0.93	0.347	0.176	3.7	4	1 row of 8 45°-slots (1.99-by-0.33)	RQL parametric test
911219	889-946	0.93	0.347	0.176	3.7	4	1 row of 8 45°-slots (1.99-by-0.33)	RQL parametric test
920123	948-994	0.88	0.87	0.15	3.7	4	1 row of 8 45°-slots (1.99-by-0.33)	Textron nozzle test
920204	999-1056	0.88	0.87	0.15	3.7	4	1 row of 8 45°-slots (1.99-by-0.33)	w/ outer fuel passage blocked

Notes:

*The outer flow *ACd* for the Textron nozzle includes the outer and the middle flow passages. The Outer *ACd* alone is 0.48.

†The *ACd* for the quick-mix flow was calculated backwards from pressure drop records. These corresponds well to sizes given in available records. The quick-mix sections used either 3/16-in. thick 5-in. ID Haynes 214 sleeves or 1/2-in. thick 4 in. ID ceramic sleeves.

‡The exact size of the slots are unknown. However, the log book entry indicated that the discharge area is the same as those of the 24 round holes in the previous runs. This is consistent with the pressure drops measured.

Table 2: Effect of Parker nozzle air circuits on RQL combustor emissions.

Rdg	P_{rb}* psia	ΔP_{34} psi	T_3 °F	ϕ_{rb}	ϕ_{ov}	T_4‡ °F	T_{rb}‡ °F	M_{rb}‡ g/mol	W_d lbm/s	W_o lbm/s	W_i lbm/s	W_q lbm/s	W_f lbm/s	J†‡	τ_{rb} ms	τ_{lb} ms	τ_{ov} ms	NO_x g/kg-f	CO g/kg-f	CO_2 %	UHC ppm	O_2 %	FARR	η %	$V_{ref,rb}$ ft/s	$V_{ref,lb}$ ft/s
598A	70.5	7.93	784	1.99	0.354	2240	2840	24.42	0.442	0.297	0.59	6.148	0.18	189.4	5.1	1.1	7.4	1.7	18	4.67	0.12	13.57	0.953	99.58	50.1	206.3
599B	70.6	8.02	784	2.00	0.356	2250	2830	24.39	0.444	0.297	0.59	6.148	0.181	188.8	5.1	1.1	7.3	1.8	10.3	4.59	0	13.58	0.953	99.76	50.2	207
600C	70.7	7.91	785	2.00	0.356	2250	2830	24.39	0.444	0.296	0.59	6.148	0.181	189	5.1	1.1	7.4	1.9	1.7	4.85	0	13.59	0.936	99.96	50.1	206.4
602A	70.1	7.6	784	2.00	0.353	2240	2830	24.4	0.443	0.205	0.676	6.169	0.18	192.3	5.1	1.1	7.3	2.1	52.7	4.55	0	13.68	0.979	98.76	50.3	207.5
603B	70	7.5	785	2.00	0.354	2240	2830	24.4	0.445	0.204	0.675	6.155	0.18	191.1	5.1	1.1	7.3	2.2	12	4.62	0	13.67	0.946	99.72	50.4	207.1
604C	69.9	7.01	783	2.00	0.354	2240	2830	24.39	0.443	0.204	0.675	6.155	0.18	191.6	5.1	1.1	7.3	2.4	2.1	4.63	0	13.62	0.941	99.95	50.3	205.6
607A	70.8	7.85	763	1.97	0.352	2210	2840	24.49	0.131	0.898	0.308	6.16	0.179	188.7	5.1	1.1	7.4	1.8	21.8	4.86	0.19	13.33	0.951	99.49	49.3	204.3
608B	71.3	8.03	760	1.97	0.353	2220	2830	24.48	0.141	0.903	0.308	6.203	0.182	186.2	5.1	1.1	7.3	2.1	7.8	4.81	0.07	13.24	0.998	99.82	49.4	204.3
609C	70.8	7.96	760	1.98	0.355	2220	2830	24.47	0.141	0.903	0.306	6.181	0.182	185.8	5	1.1	7.3	2.4	1.7	4.52	0.14	13.52	0.986	99.96	49.7	204.8
611A	71.4	7.64	763	1.98	0.352	2210	2830	24.46	0.139	0.794	0.398	6.17	0.179	190.8	5.2	1.1	7.5	1.7	16.3	4.78	0	13.39	0.942	99.62	48.7	201.8
612B	71.1	7.99	764	1.98	0.351	2210	2830	24.47	0.142	0.794	0.398	6.174	0.179	190.1	5.1	1.1	7.4	2	8	4.66	0	13.52	0.988	99.81	49.1	204.2
613C	71.3	7.95	766	1.97	0.351	2220	2850	24.51	0.151	0.793	0.397	6.164	0.179	187.9	5.1	1.1	7.4	2.5	1.7	4.49	0	13.64	0.961	99.96	49.2	203.9
615A	70.5	7.03	762	2.00	0.353	2220	2800	24.39	0.126	0.61	0.591	6.186	0.18	193.9	5.1	1.1	7.4	1.4	11.4	4.64	0.21	13.26	0.926	99.73	49.2	203.6
616B	70.5	6.98	759	1.99	0.353	2210	2820	24.44	0.131	0.61	0.593	6.193	0.18	191.4	5.1	1.1	7.4	1.5	8.3	4.59	0.24	13.37	0.971	99.8	49.3	202.9
617C	70.3	6.94	763	1.98	0.352	2220	2830	24.47	0.136	0.61	0.593	6.169	0.18	188.9	5	1.1	7.4	1.9	0.2	4.52	0.19	13.42	0.956	99.99	49.7	202.9
619A	70	6.27	761	1.98	0.351	2210	2830	24.46	0.134	0.408	0.79	6.193	0.179	192	5	1.1	7.4	1.3	29.2	4.67	0.19	13.4	0.949	99.31	49.6	202
620B	70	6.96	762	1.99	0.354	2220	2810	24.41	0.135	0.407	0.79	6.167	0.181	191	5.1	1.1	7.4	1.2	10.1	4.52	0.17	13.42	0.969	99.76	49.7	204
621C	69.9	6.24	761	1.99	0.355	2220	2810	24.42	0.138	0.408	0.79	6.167	0.181	189.8	5	1.1	7.4	1.5	1.7	4.34	0.24	13.54	0.941	99.96	49.9	201.8
623A	69.9	7.04	762	2.01	0.356	2230	2800	24.37	0.137	0.276	0.917	6.167	0.182	191.6	5.1	1.1	7.4	1.1	37.2	4.58	0.14	13.37	0.903	99.12	49.8	204.7
624B	69.7	6.35	761	1.99	0.354	2220	2820	24.43	0.141	0.276	0.921	6.193	0.181	190.5	5	1.1	7.3	1.3	10.7	4.6	0.1	13.51	0.962	99.75	50.1	203.1
625C	69.9	5.8	764	1.98	0.354	2220	2830	24.45	0.142	0.276	0.92	6.169	0.18	189	5	1.1	7.3	1.6	7.2	4.57	0.07	13.58	0.95	99.83	50.1	201.4
627A	70.3	7.05	781	2.00	0.354	2240	2820	24.38	1.078	0.181	0.071	6.193	0.181	192	5.1	1.1	7.4	2.9	42.8	4.73	0.23	19.89	0.941	98.99	50.2	205.9
628B	70.6	6.92	780	2.01	0.354	2240	2820	24.37	1.076	0.18	0.071	6.186	0.181	192.5	5.1	1.1	7.4	2.5	9.9	4.83	0.16	13.64	0.742	99.77	49.9	203.6
629C	70.9	7.84	780	2.00	0.354	2240	2820	24.39	1.079	0.18	0.071	6.193	0.181	191.8	5.1	1.1	7.4	2.9	2.2	4.76	0.17	13.75	0.972	99.95	49.8	205.8
631A	69.8	6.95	780	2.00	0.359	2260	2820	24.38	1.077	0.163	0.076	6.038	0.179	186.6	5.1	1.1	7.4	2.2	27.4	4.92	0.19	13.49	0.944	99.36	50	201.8
632B	69.9	7.46	780	2.00	0.358	2250	2820	24.39	1.079	0.163	0.076	6.058	0.179	186.8	5.1	1.1	7.4	2.5	8.3	4.9	0.14	13.42	0.987	99.8	50	204
633C	70	7.08	779	2.00	0.358	2250	2820	24.39	1.08	0.163	0.077	6.058	0.179	186.6	5.1	1.1	7.4	2.8	2.1	4.86	0.14	13.47	0.98	99.95	50	202.4
635A	70.4	7.72	779	1.99	0.358	2250	2830	24.41	1.08	0.124	0.119	6.056	0.179	185.6	5.1	1.1	7.4	2.4	26.8	4.87	0.16	13.33	0.973	99.37	49.8	203.1
636B	70.8	7.28	779	2.00	0.359	2250	2820	24.4	1.08	0.125	0.119	6.056	0.18	185.3	5.1	1.1	7.4	2.6	9.1	4.87	0.19	13.38	0.986	99.79	49.6	200.6
637C	70.1	8.08	779	2.00	0.358	2250	2820	24.4	1.081	0.124	0.119	6.058	0.18	185.3	5.1	1.1	7.3	2.9	2.1	4.8	0.21	13.39	0.977	99.95	50.1	205.1
639A	70.5	7.31	776	2.01	0.36	2260	2800	24.34	1.08	0.077	0.16	6.056	0.181	187.6	5.1	1.1	7.5	2.4	24.5	5.02	0.23	13.16	0.962	99.42	49.4	201.4
640B	71.6	7.59	775	1.99	0.355	2240	2830	24.44	1.08	0.079	0.16	6.065	0.178	187	5.2	1.1	7.6	2.7	8.1	4.84	0.26	13.19	1.022	99.81	48.6	198.4
641C	70.9	7.28	775	1.98	0.354	2240	2840	24.45	1.081	0.08	0.16	6.075	0.178	187.1	5.1	1.1	7.5	3.1	2.2	4.72	0.23	13.35	0.993	99.95	49.2	200
643A	71.4	7.9	772	2.00	0.358	2240	2820	24.4	1.08	0.057	0.188	6.073	0.18	186.4	5.2	1.1	7.5	2.2	18.5	4.96	0.14	13.17	0.959	99.57	48.9	200.8
644B	71.2	7.27	772	2.00	0.359	2250	2810	24.39	1.079	0.055	0.188	6.056	0.18	186.2	5.2	1.1	7.5	2.5	7.5	4.88	0.16	13.28	1.002	99.82	48.9	198.4
645C	70.5	7.22	772	2.00	0.358	2240	2820	24.39	1.077	0.054	0.188	6.056	0.179	187	5.1	1.1	7.5	3	1.9	4.82	0.17	13.29	0.984	99.95	49.3	200.5
660A	70.3	7.49	586	1.98	0.355	2050	2650	24.46	0.141	0.403	0.795	6.141	0.18	197.7	5.3	1.2	7.8	1.5	12.8	4.91	0.61	13.63	0.984	99.7	42.6	190.4
662A	70	7.79	585	2.00	0.358	2060	2630	24.41	0.141	0.276	0.92	6.124	0.181	197.6	5.3	1.2	7.7	1.6	10.2	4.93	0.47	13.63	0.975	99.76	42.7	191.7
664A	70.1	7.22	598	1.99	0.355	2060	2660	24.44	0.266	0.246	0.82	6.124	0.18	198.1	5.3	1.2	7.8	1.7	11.8	4.91	0.51	13.73	0.985	99.72	43	190.2
666A	71.7	5.86	600	1.99	0.358	2070	2660	24.44	0.26	0.718	0.345	6.022	0.179	194.1	5.5	1.3	8.1	2.3	6.2	5.25	0.28	13.54	0.97	99.85	41.8	178.6
668A	70.8	7.85	573	2.00	0.356	2040	2610	24.38	0.088	0.29	0.95	6.139	0.181	202.5	5.5	1.2	7.9	1.7	12.9	5.22	0.37	13.38	1.025	99.7	41.4	188.4

Table 2 (Concluded.)

Rdg	P_{rb}* psia	ΔP_{34} psi	T_3 °F	ϕ_{rb}	ϕ_{ov}	T_4‡ °F	T_{rb}‡ °F	M_{rb}‡ g/mol	W_d lbm/s	W_o lbm/s	W_i lbm/s	W_q lbm/s	W_f lbm/s	J†‡	τ_{rb} ms	τ_{lb} ms	τ_{ov} ms	NO_x g/kg-f	CO g/kg-f	CO_2 %	UHC ppm	O_2 %	FARR	η %	$V_{ref,rb}$ ft/s	$V_{ref,lb}$ ft/s
670A	70.3	7.76	605	2.00	0.358	2080	2650	24.41	1.201	0.122	0.069	6.362	0.189	195	5.1	1.1	7.4	2.5	8.4	5.33	0.28	13.43	1.024	99.8	45.1	199.5
672A	71.6	6.55	606	2.00	0.355	2070	2650	24.4	0.439	0.296	0.582	6.081	0.179	199.3	5.5	1.2	8	2.2	8.8	5.11	0.19	13.65	1.043	99.79	41.9	182.9
675A	71.5	11	714	2.00	0.565	2890	2760	24.4	0.191	0.463	1.274	4.886	0.262	66.1	3.6	0.9	5.2	4.5	18.7	7.71	0.27	10.3	0.631	99.56	67.7	203.3
676B	69.2	8.69	716	2.03	0.573	2920	2720	24.29	0.188	0.463	1.271	4.884	0.265	66.7	3.5	0.9	5.1	4.2	19.6	7.8	0.11	10.19	0.921	99.54	70	203.2
680A	72	8.65	741	1.99	0.591	3000	2790	24.41	0.243	0.668	1.252	5.14	0.293	58.6	3.2	0.9	4.7	3.2	18.8	7.75	0.15	8.67	0.902	99.56	77.2	213
681B	72.6	8.47	742	1.99	0.59	3000	2800	24.43	0.245	0.669	1.25	5.14	0.293	58.4	3.2	0.9	4.7	3.6	12.4	7.62	0.25	8.49	0.97	99.71	76.6	210.4
683C	72.7	8.9	743	2.00	0.589	3000	2790	24.4	0.246	0.671	1.248	5.174	0.294	59.2	3.3	0.9	4.7	3.9	13	7.76	0	8.76	0.971	99.7	76.6	212.2

*P_{rb} originally was P_3 listed at 100 psia.

†The J values tabulated here are computed based on a 5-in. ID quick-mix section with 8 45° slanted slots of 0.33 by 1.99 in. area each. The J values listed by the original manuscript were about 3 times smaller.

‡Estimated

Table 3: Effect of Textron nozzle air and fuel circuits on RQL combustor emissions

Rdg	P_{rb} psia	ΔP_{34} psi	T_3 °F	ϕ_{rb}	ϕ_{ov}	T_4‡ °F	T_{rb}‡ °F	M_{rb}‡ g/mol	W_d lbm/s	W_o† lbm/s	W_i lbm/s	W_q lbm/s	W_f* lbm/s	J‡	τ_{rb} ms	τ_{lb} ms	τ_{ov} ms	NO_x g/kg-fg/kg-f	CO	CO_2 %	UHC ppm	O_2 %	FARR	η %	$V_{ref,rb}$ ft/s	$V_{ref,lb}$ ft/s
951A	121	13.7	790	1.98	0.357	2260	2850	24.45	0.774	0.734	0.13	7.461	0.221	59.6	7	1.5	9.6	3.3	13.9	3.85	2.59	14.54	1.43	99.67	36.2	147.6
952B	121	13.6	790	1.99	0.358	2260	2840	24.43	0.772	0.731	0.13	7.448	0.221	59.8	7.1	1.5	9.6	3.7	19.3	4.31	1.29	13.71	0.79	99.54	36.1	147.3
953C	122	14	790	1.99	0.358	2260	2850	24.43	0.773	0.728	0.129	7.434	0.221	59.7	7.1	1.5	9.7	3.9	1.7	5.06	2.22	12.84	0.893	99.96	35.7	147.1
955A	123	14.1	789	1.99	0.358	2260	2850	24.44	0.77	0.771	0.094	7.445	0.221	59.4	7.2	1.5	9.8	3.3	46.5	3.95	1.54	14.24	1.029	98.9	35.5	145.8
956B	124	15	789	2.01	0.363	2280	2810	24.34	0.773	0.771	0.094	7.45	0.225	59.5	7.2	1.5	9.8	3.6	18.3	4.4	0.83	13.51	0.813	99.57	35.3	146
957C	124	14.1	791	2.01	0.363	2280	2820	24.36	0.771	0.773	0.095	7.436	0.224	59.4	7.2	1.5	9.8	3.9	1.4	5.07	0.82	12.46	0.9	99.97	35.4	144.6
959A	122	13.6	787	1.99	0.359	2260	2840	24.41	0.771	0.684	0.179	7.448	0.222	59.6	7.1	1.5	9.7	3.3	48	3.97	0.6	14.04	1.047	98.87	35.7	145.7
960B	122	13.7	787	1.99	0.359	2260	2840	24.41	0.771	0.684	0.179	7.448	0.222	59.6	7.1	1.5	9.7	3.6	21.2	4.38	0.6	13.41	0.834	99.5	35.7	145.7
961C	122	13.9	791	1.99	0.359	2270	2840	24.41	0.771	0.68	0.179	7.42	0.221	59.7	7.1	1.5	9.7	3.8	0.9	5.04	0.36	12.37	0.912	99.98	35.7	147
963A	123	15.1	789	1.99	0.355	2250	2840	24.43	0.771	0.429	0.426	7.494	0.22	61	7.2	1.5	9.8	3	47.1	4.07	0.48	14.8	1.061	98.89	35.3	146.4
964B	123	14.6	787	1.99	0.355	2250	2840	24.42	0.77	0.429	0.425	7.491	0.22	61	7.2	1.5	9.8	3.4	20.3	4.44	0.48	14.17	0.825	99.52	35.2	146.1
965C	123	14.2	787	1.99	0.355	2250	2840	24.43	0.771	0.428	0.425	7.488	0.22	61	7.2	1.5	9.8	3.7	1.5	5.05	0.36	13.32	0.898	99.96	35.2	146.2
967A	123	8.33	783	1.98	0.358	2260	2850	24.46	0.39	1.067	0.182	7.422	0.221	59	7.2	1.6	9.9	3.3	10.6	5.4	1.17	12.14	1.004	99.75	35.4	137.7
968B	127	11.4	784	1.98	0.359	2260	2850	24.46	0.391	1.065	0.182	7.392	0.221	58.7	7.4	1.6	10.2	3.5	4.8	4.76	0.83	12.98	1.107	99.89	34.3	136.1
969C	126	12.4	786	1.97	0.358	2260	2860	24.5	0.391	1.07	0.182	7.409	0.22	58.6	7.3	1.6	10	3.7	0.5	4.74	1.17	13.08	0.985	99.98	34.7	139.1
971A	122	12.4	784	2.00	0.36	2260	2830	24.41	0.39	1.118	0.13	7.449	0.222	59.7	7.1	1.6	9.7	3.1	3.4	5.33	0.82	12.24	0.97	99.92	35.7	144.6
972B	121	11.2	786	1.97	0.355	2250	2860	24.49	0.391	1.12	0.131	7.468	0.22	59.6	7	1.6	9.6	3.4	4.5	4.73	0.59	13.08	1.104	99.89	36.1	145.1
973C	121	11.6	781	1.98	0.358	2250	2840	24.45	0.388	1.121	0.131	7.447	0.221	59.3	7	1.6	9.7	3.4	0.9	4.78	0.71	13.26	0.975	99.98	36	144.2
975A	122	11.8	782	2.01	0.359	2260	2810	24.35	0.388	0.972	0.256	7.425	0.221	60.9	7.2	1.6	9.9	3.1	10.3	5.26	0.36	12.53	0.967	99.76	35.2	143.5
976B	122	11.7	781	2.00	0.358	2250	2830	24.4	0.389	0.978	0.257	7.445	0.221	60.5	7.2	1.6	9.8	3.4	5.3	4.73	0.59	13.27	1.073	99.87	35.3	143.8
977C	122	12	779	2.01	0.359	2260	2810	24.36	0.391	0.979	0.258	7.475	0.222	60.8	7.2	1.6	9.8	3.4	0.8	4.81	0.48	13.35	0.961	99.98	35.4	144.2
979A	122	10.8	784	1.98	0.357	2260	2850	24.47	0.394	0.629	0.622	7.46	0.221	59.3	7.1	1.6	9.7	2.8	9.9	5.1	0.36	12.93	0.972	99.77	35.8	143.5
980B	122	10.6	783	1.97	0.356	2250	2860	24.49	0.393	0.63	0.624	7.494	0.221	59.6	7.1	1.6	9.7	2.9	5.5	4.73	0.48	13.56	1.039	99.87	35.8	144
982A	118	9.79	790	1.97	0.356	2260	2870	24.49	0.982	0.562	0.105	7.482	0.221	59.1	6.8	1.5	9.4	3.6	11.7	4.93	0.36	13.34	0.957	99.72	37.3	146.7
983B	120	11.7	790	1.99	0.359	2270	2850	24.44	0.981	0.561	0.104	7.469	0.222	59.1	6.9	1.5	9.5	4.2	3.7	4.7	0.48	13.66	0.989	99.91	36.7	146.5
985A	121	12.2	789	2.00	0.359	2260	2830	24.4	0.974	0.59	0.073	7.482	0.222	60.1	7.1	1.5	9.6	4	11.5	4.77	0.59	13.74	0.941	99.73	36.1	146.5
986B	121	12.7	789	1.99	0.356	2260	2850	24.43	0.974	0.59	0.072	7.496	0.221	60.3	7.1	1.5	9.6	4.2	3.5	4.81	0.24	13.74	0.955	99.92	36.1	148.1
987A	122	12.1	790	2.00	0.36	2270	2830	24.38	0.972	0.514	0.137	7.416	0.221	60.1	7.2	1.6	9.8	3.9	10.7	4.83	0.48	13.64	0.949	99.75	35.6	143.9
988A	122	11.6	791	1.99	0.357	2260	2840	24.42	0.978	0.517	0.138	7.479	0.221	60.3	7.1	1.6	9.7	3.9	10.7	4.83	0.48	13.73	0.965	99.75	35.8	145.2
989B	122	12.1	791	1.99	0.358	2260	2840	24.41	0.977	0.517	0.138	7.463	0.221	60.2	7.1	1.6	9.8	4.1	3.4	4.7	0.48	13.85	0.96	99.92	35.8	143.7
991A	118	13.2	830	1.77	0.361	2320	3160	25.29	0.872	0.581	0.382	7.162	0.221	43.9	5.9	1.5	8.3	3.2	5.4	5.37	0.36	12.9	0.926	99.87	42.3	153.5
992A	118	13.7	830	2.00	0.408	2480	2870	24.39	0.719	0.668	0.44	7.118	0.248	44.5	6.1	1.4	8.3	3.1	7.6	5.36	0.24	13	0.934	99.82	42.7	154.2
993A	119	13.1	827	2.00	0.407	2480	2870	24.4	0.643	0.722	0.468	7.154	0.249	44.6	6.1	1.4	8.4	3	7.2	5.45	0.47	12.98	0.932	99.83	42.4	153
994B	119	13	827	2.00	0.408	2480	2870	24.39	0.643	0.719	0.468	7.14	0.249	44.6	6.1	1.4	8.4	3.4	1.5	5.58	0.47	12.68	0.94	99.96	42.3	152.7
1002A	123	16.1	783	1.98	0.358	2260	2850	24.45	0.386	1.117	0.134	7.434	0.221	59.3	7.2	1.5	9.7	3.4	25.7	4.34	0	13.8	1.101	99.4	35.4	148.2
1003A	122	16.6	783	1.97	0.357	2250	2860	24.49	0.389	1.119	0.135	7.431	0.22	58.9	7.1	1.5	9.6	3.3	22.7	4.33	0	13.8	0.896	99.47	35.7	149.7
1004B	123	16.7	783	1.97	0.357	2250	2860	24.49	0.39	1.126	0.135	7.472	0.221	59	7.1	1.5	9.6	3.7	9.1	4.59	0.28	13.38	0.894	99.78	35.6	150.5
1005C	120	17.2	782	1.98	0.359	2260	2850	24.47	0.39	1.122	0.135	7.434	0.221	58.7	7	1.5	9.4	3.8	3	4.78	0.35	13.26	0.941	99.93	36.4	154.1
1007A	119	22.5	784	1.99	0.355	2250	2840	24.43	0.389	0.978	0.257	7.472	0.22	61	7	1.4	9.3	3.7	7.4	4.77	0.49	13.65	0.98	99.83	36.3	164.2
1008B	119	22.4	784	1.99	0.356	2250	2840	24.44	0.391	0.979	0.257	7.458	0.22	60.6	7	1.4	9.3	3.8	6.8	4.72	0.3	13.75	0.96	99.84	36.3	164.1
1011A	119	23.2	784	1.99	0.356	2250	2840	24.43	0.389	0.622	0.616	7.458	0.22	60.5	7	1.4	9.3	2.8	3.3	5.39	0.16	13.09	0.947	99.92	36.4	165.9

Table 3: (Concluded.)

Rdg	P_{rb} psia	ΔP_{34} psi	T_3 °F	ϕ_{rb}	ϕ_{ov}	T_4‡ °F	T_{rb}‡ °F	M_{rb}‡ g/mol	W_d lbm/s	W_o† lbm/s	W_i lbm/s	W_q lbm/s	W_f* lbm/s	J‡	τ_{rb} ms	τ_{lb} ms	τ_{ov} ms	NO_x g/kg-f	CO g/kg-f	CO_2 %	UHC ppm	O_2 %	FARR	η %	$V_{ref,rb}$ ft/s	$V_{ref,lb}$ ft/s
1013B	120	22.6	783	1.99	0.356	2250	2840	24.42	0.389	0.619	0.616	7.458	0.22	60.8	7.1	1.4	9.4	2.8	1.9	5.34	1.06	13.57	1.063	99.95	36	163
1014B	120	22.6	783	2.00	0.358	2260	2830	24.39	0.389	0.619	0.616	7.458	0.221	60.8	7.1	1.4	9.4	2.7	1.9	5.38	1.06	13.56	1.029	99.95	36	163.4
1015C	120	22.3	784	2.00	0.359	2260	2820	24.38	0.389	0.619	0.615	7.428	0.221	60.5	7.1	1.4	9.4	3.1	1.2	5.09	1.09	13.89	1.03	99.97	36	162.4
1017A	120	22.4	785	1.99	0.358	2260	2840	24.43	0.39	1.064	0.181	7.455	0.221	60	7	1.4	9.3	3.3	4.4	5.14	0.24	13.31	0.983	99.9	36.3	163
1018B	120	22.5	783	1.99	0.358	2260	2830	24.41	0.389	1.063	0.181	7.455	0.222	60.1	7	1.4	9.3	3	2.5	5.63	0.36	12.68	1.016	99.94	36.2	163.1
1019C	120	22.4	784	1.99	0.359	2260	2830	24.41	0.391	1.065	0.181	7.458	0.222	59.8	7	1.4	9.3	3.5	1.7	5.07	0.24	13.41	1.105	99.96	36.3	162.8
1021A	120	22.6	783	2.00	0.358	2260	2830	24.4	0.389	1.111	0.134	7.485	0.222	60.5	7	1.4	9.4	2.9	1.9	5.68	0.36	12.58	1.002	99.95	36.2	162.7
1022B	119	22.9	783	2.00	0.359	2260	2830	24.4	0.391	1.11	0.134	7.472	0.222	60.2	7	1.4	9.3	3.1	3	5.33	0.36	13.19	1.118	99.93	36.5	164.8
1023C	120	22.6	783	2.00	0.358	2260	2830	24.41	0.391	1.113	0.134	7.485	0.222	60.3	7	1.4	9.3	3.4	1.4	5.09	0.01	13.51	1.046	99.97	36.3	163.4
1025A	121	23.4	791	1.98	0.355	2250	2850	24.45	0.77	0.725	0.135	7.485	0.22	60.6	7.1	1.4	9.4	3.5	5.4	4.76	0.36	13.27	1.009	99.87	36	162.8
1026A	123	24.7	791	1.98	0.355	2250	2850	24.45	0.768	0.727	0.135	7.472	0.22	60.4	7.2	1.4	9.5	3.5	7	4.5	1.23	13.59	0.978	99.83	35.4	162.7
1027B	122	24.6	791	1.99	0.356	2260	2850	24.44	0.768	0.725	0.134	7.458	0.22	60.4	7.1	1.4	9.5	3.4	5.7	4.68	1.21	13.37	0.926	99.86	35.7	163.6
1028C	122	24.5	791	1.99	0.355	2250	2850	24.44	0.768	0.725	0.135	7.485	0.22	60.8	7.1	1.4	9.5	3.7	1.7	4.81	1.19	13.16	0.962	99.96	35.7	163.9
1030A	123	24.6	791	1.98	0.356	2260	2850	24.45	0.77	0.77	0.092	7.445	0.22	59.8	7.2	1.4	9.5	3.3	4	4.86	1.28	13.16	0.984	99.9	35.5	161.9
1031B	122	25	790	1.98	0.357	2260	2850	24.45	0.77	0.767	0.092	7.431	0.22	59.7	7.1	1.4	9.4	3.4	3.4	4.79	1.23	13.36	0.991	99.92	35.7	164
1033C	122	25.1	791	1.99	0.357	2260	2850	24.43	0.772	0.769	0.092	7.477	0.221	60.2	7.1	1.4	9.4	3.5	1.4	4.8	1.19	13.36	0.973	99.96	35.8	164.3
1036A	123	25.5	791	1.99	0.356	2260	2850	24.43	0.768	0.676	0.18	7.458	0.22	60.6	7.2	1.4	9.5	3.4	5.2	4.73	1.7	13.56	0.975	99.87	35.3	163.7
1037B	122	25.2	792	1.99	0.356	2260	2850	24.43	0.769	0.674	0.18	7.458	0.22	60.7	7.2	1.4	9.5	3.6	3.7	4.8	1.31	13.45	0.957	99.91	35.6	163.4
1038C	122	25.6	792	1.99	0.356	2260	2850	24.43	0.769	0.676	0.18	7.458	0.22	60.5	7.2	1.4	9.5	3.7	1.8	4.79	1.23	13.55	0.971	99.96	35.7	164.3
1040A	124	25.7	792	2.00	0.358	2260	2830	24.38	0.77	0.429	0.424	7.458	0.221	60.8	7.3	1.4	9.6	4	2	5.21	1.16	13.11	0.96	99.95	35.1	161.4
1041A	124	26.6	792	2.00	0.359	2270	2830	24.38	0.769	0.429	0.424	7.442	0.221	60.6	7.3	1.4	9.6	4.1	2.4	4.97	1.21	13.33	1.032	99.94	35	163.4
1042B	124	26.4	792	2.00	0.358	2270	2830	24.38	0.768	0.429	0.424	7.445	0.221	60.8	7.3	1.4	9.6	4.3	1	4.78	1.14	13.64	0.993	99.97	35	162.1
1044A	120	27.4	792	1.99	0.357	2260	2840	24.42	0.969	0.553	0.104	7.453	0.22	60.4	7	1.3	9.3	3.4	2.9	5.25	1.35	13.01	0.957	99.93	36.3	171.4
1045B	120	27.7	792	2.00	0.359	2270	2840	24.4	0.97	0.552	0.104	7.431	0.221	60.1	7	1.3	9.2	3.5	3.7	5.03	1.26	13.33	1.043	99.91	36.3	171.7
1046C	120	27.8	792	1.99	0.356	2260	2850	24.43	0.969	0.551	0.104	7.445	0.22	60.4	7	1.3	9.3	3.8	2.2	4.8	1.19	13.74	1.006	99.95	36.2	172.1
1048A	120	28.3	793	1.99	0.358	2270	2850	24.42	0.972	0.517	0.141	7.445	0.221	59.9	7	1.3	9.2	3.4	3.4	5.14	1.16	13.12	0.952	99.92	36.4	173.2
1049B	124	25.9	793	1.99	0.356	2260	2850	24.44	0.969	0.517	0.141	7.445	0.22	60.1	7.3	1.4	9.6	3.7	3.9	4.91	1.16	13.53	1.031	99.91	35.1	162.1
1050C	123	25.8	793	2.06	0.358	2270	2770	24.2	0.971	0.459	0.142	7.453	0.22	65.2	7.5	1.4	9.9	3.9	2.4	4.83	1.23	13.73	0.976	99.94	34.3	162.1
1052A	120	28.1	793	2.00	0.36	2270	2830	24.39	0.968	0.332	0.331	7.431	0.222	59.7	7	1.3	9.2	5	3.2	5.34	1.11	13	0.95	99.92	36.4	173.2
1053A	120	27.9	793	2.00	0.36	2270	2830	24.38	0.967	0.332	0.331	7.431	0.222	59.8	7	1.3	9.2	5.1	3.2	5.28	1.14	12.91	1.05	99.92	36.4	172
1054B	120	28.2	792	2.00	0.36	2270	2830	24.39	0.968	0.332	0.331	7.44	0.222	59.9	7	1.3	9.2	5.2	3.9	5.04	1.19	13.32	1.047	99.91	36.4	172.5
1055B	120	27.8	792	2.00	0.361	2280	2830	24.39	0.968	0.333	0.33	7.417	0.222	59.5	7	1.3	9.2	5.6	4.1	4.6	1.21	13.38	0.996	99.9	36.4	171.7
1056C	120	27.9	793	2.00	0.36	2270	2840	24.39	0.97	0.333	0.33	7.431	0.222	59.6	7	1.3	9.2	5.4	2.8	4.86	1.19	13.73	0.936	99.93	36.5	172.4

*Fuel flow (W_f) through the Textron nozzle is total. In Rdgs. 948-994, about 60% of the fuel flow through the outer fuel passage. The outer passage was blocked for Rdgs. 999-1056.

†The outer airflow, W_o, shown above is W_o+W_m

‡Estimated

Table 4. RQL combustion parametric data with Parker nozzle.

Rdg	P_{rb} psia	ΔP_{34} psi	T_3 °F	ϕ_{rb}	ϕ_{ov}	T_4‡ °F	T_{rb}‡ °F	M_{rb}‡ g/mol	W_d lbm/s	W_o lbm/s	W_i lbm/s	W_q lbm/s	W_f lbm/s	J‡	τ_{rb} ms	τ_{lb} ms	τ_{ov} ms	NO_x g/kg-f	CO g/kg-f	CO_2 %	UHC ppm	O_2 %	FARR	η %	$V_{ref,rb}$ ft/s	$V_{ref,lb}$ ft/s
764A	119	11.4	821	2.00	0.41	2480	2860	24.38	0.405	0.722	0.709	7.151	0.25	44.6	6.1	1.4	8.4	3.3	13.6	2.97	0.13	13.09	1.388	99.68	42.3	150
765B	119	12	820	2.01	0.411	2480	2850	24.34	0.407	0.722	0.71	7.17	0.252	44.7	6.1	1.4	8.4	3.4	2.2	3.61	0.48	12.31	0.614	99.95	42.3	151.5
766C	119	11.6	819	2.01	0.41	2480	2850	24.37	0.408	0.725	0.709	7.17	0.251	44.5	6.1	1.4	8.4	4.9	0.5	4.04	0	12.06	0.738	99.99	42.4	150.2
767A	123	13	828	1.99	0.402	2460	2880	24.42	0.799	0.502	0.567	7.397	0.253	45.9	6.2	1.4	8.5	3.4	11.5	4	0	13.25	0.824	99.73	41.8	152.1
768B	120	12.4	831	1.95	0.398	2450	2930	24.56	0.784	0.491	0.554	7.154	0.243	44.7	6.1	1.4	8.5	3.7	2.5	4.02	0	12.72	0.779	99.94	42	150.6
769C	118	11.8	832	2.06	0.422	2530	2800	24.19	0.778	0.487	0.549	7.052	0.254	44.6	6.2	1.4	8.4	4.3	0.5	4.78	1.17	12.48	0.756	99.99	42.7	150.2
770A	117	12.4	823	2.03	0.417	2500	2830	24.3	0.402	0.488	0.914	6.973	0.249	44.1	6.2	1.4	8.4	2.6	11.7	4.29	0.6	13.72	0.868	99.72	42.4	150.9
771B	117	12.6	825	2.03	0.415	2500	2840	24.3	0.403	0.489	0.913	7.012	0.249	44.6	6.2	1.4	8.4	2.8	2.1	4.63	0.48	13.26	0.765	99.95	42.5	151.8
772C	116	12	827	2.00	0.419	2520	2870	24.39	0.406	0.493	0.922	6.868	0.247	41.9	6	1.4	8.2	3.2	0.5	4.99	0.24	13.26	0.814	99.99	43.2	151.2
773A	148	7.37	821	2.02	0.417	2500	2840	24.32	0.376	0.666	0.659	6.555	0.234	43.7	8.3	2	11.4	3.3	3.8	4.64	0.01	14.2	0.858	99.91	31.5	106
774B	151	7.76	817	2.03	0.412	2480	2830	24.31	0.379	0.671	0.664	6.714	0.236	45.2	8.4	2	11.6	3.6	1.1	4.67	0.13	13.86	0.792	99.97	31.1	105.7
776C	148	7.66	820	2.05	0.422	2520	2800	24.22	0.378	0.665	0.657	6.568	0.237	44.1	8.3	2	11.5	4	0.4	4.93	0.13	13.41	0.789	99.99	31.5	105.3
778A	152	16.4	823	1.97	0.399	2440	2910	24.51	0.498	0.885	0.877	8.879	0.302	45.2	6.3	1.5	8.7	2.9	9.7	4.65	0.01	14.56	0.884	99.77	40.7	147.4
779B	151	15.9	825	2.03	0.412	2490	2830	24.29	0.495	0.882	0.872	8.826	0.311	45.4	6.4	1.4	8.7	3.3	2.1	4.63	0	13.77	0.781	99.95	41	147.9
785A	122	10.2	598	2.01	0.482	2500	2630	24.36	0.817	0.522	0.561	6.014	0.26	25.9	6.5	1.7	9	2.4	23.5	5.44	1.17	11.9	0.689	99.44	35.2	104.6
786B	121	10.5	595	2.00	0.481	2500	2630	24.38	0.818	0.524	0.561	6.02	0.259	25.8	6.5	1.6	8.9	2.9	2.8	5.74	0.7	11.48	0.845	99.93	35.5	105.4
788A	121	10.3	591	2.00	0.479	2490	2630	24.39	0.417	0.749	0.739	6.054	0.259	26.1	6.5	1.6	8.9	2	25.5	5.41	1.05	11.99	0.888	99.4	35.4	105.7
789B	121	9.19	590	2.00	0.479	2480	2640	24.4	0.416	0.75	0.737	6.039	0.258	25.9	6.5	1.7	9	2.7	3.3	5.69	0.82	11.44	0.842	99.92	35.3	103.5
790C	121	10.2	591	2.00	0.479	2480	2630	24.39	0.415	0.75	0.738	6.057	0.259	26.1	6.5	1.6	9	3.1	0.5	6.07	1.05	10.9	0.887	99.99	35.3	105.6
793A	122	4.59	587	1.99	0.48	2490	2640	24.42	0.276	0.506	0.501	4.042	0.174	25.6	9.7	2.6	13.6	2.4	65.7	5.03	5.93	11.75	0.94	98.44	23.6	66.3
795B	118	3.93	588	1.99	0.479	2480	2640	24.43	0.276	0.505	0.501	4.042	0.174	25.6	9.3	2.5	13.2	3.6	1.7	5.76	0.82	11.9	0.824	99.96	24.3	68.1
796A	151	3.98	586	2.00	0.48	2490	2630	24.39	0.355	0.63	0.617	5.073	0.218	25.8	9.6	2.6	13.5	3.1	56	5.88	4.27	11.56	0.869	98.67	23.7	66.5
797B	150	3.72	589	2.01	0.484	2500	2620	24.36	0.354	0.629	0.617	5.044	0.219	25.6	9.6	2.6	13.5	4.2	1.8	5.9	0.82	11.79	0.901	99.96	23.9	66.4
798A	81.9	12.9	588	2.01	0.482	2490	2630	24.38	0.382	0.678	0.66	5.437	0.235	25.7	4.8	1.1	6.6	1.4	80.6	5.66	2.09	11.92	0.882	98.1	47.1	151.9
799B	81.3	14.1	590	2.01	0.483	2500	2620	24.36	0.383	0.678	0.66	5.434	0.235	25.7	4.8	1.1	6.5	1.4	10.3	5.93	0.7	11.84	0.872	99.76	47.6	156.1
801A	79.7	6.89	587	2.01	0.494	2530	2620	24.36	0.295	0.518	0.506	4.049	0.18	24.3	6.2	1.6	8.5	1.6	76.6	5.67	3.01	12.01	0.865	98.19	37	107.8
802B	79.6	6.44	585	1.98	0.487	2510	2650	24.46	0.295	0.517	0.503	4.037	0.177	24.2	6.1	1.6	8.6	2	4.9	5.81	0.36	12.09	0.862	99.88	36.9	107.1
803A	119	9.62	588	2.00	0.431	2320	2640	24.41	0.372	0.673	0.666	6.219	0.232	34	7.1	1.7	9.8	2.2	32.1	4.93	0.59	13.58	0.966	99.24	32.2	106.1
804B	119	9.11	588	2.00	0.431	2320	2630	24.4	0.371	0.674	0.666	6.226	0.233	34.1	7.1	1.7	9.8	2.6	6.3	5.23	0.36	13.18	0.819	99.85	32.2	106.2
813A	121	7.26	819	2.00	0.412	2480	2870	24.4	0.312	0.531	0.541	5.333	0.188	43.6	8.3	2	11.5	3.4	7.1	5.02	11.23	12.85	0.9	99.81	31.3	106.1
814B	119	7.22	819	1.99	0.412	2480	2870	24.41	0.313	0.532	0.541	5.333	0.188	43.5	8.1	2	11.3	3.7	1.3	5.35	5.33	12.33	0.891	99.96	31.9	108
819A	122	5.09	819	1.99	0.451	2620	2870	24.41	0.297	0.533	0.531	4.659	0.185	34.4	8.5	2.2	11.9	3.7	5.7	5.63	3.24	12.2	0.867	99.86	30.5	92.6
820B	123	5.14	818	2.00	0.453	2630	2860	24.38	0.298	0.534	0.531	4.666	0.186	34.5	8.5	2.2	12	4.1	0.8	6.39	2.41	11.73	0.896	99.98	30.3	91.9
822A	121	4.38	818	2.03	0.518	2840	2820	24.29	0.296	0.536	0.534	3.987	0.189	25.2	8.4	2.3	11.8	3.6	9.9	6.74	1.95	11.13	0.861	99.76	30.9	82.3
823B	120	4.69	818	2.02	0.516	2840	2830	24.31	0.295	0.536	0.534	3.991	0.188	25.2	8.4	2.3	11.7	4.7	1.1	6.71	1.96	10.67	0.918	99.97	31.2	83.1
825A	123	8.87	821	1.99	0.51	2820	2870	24.42	0.399	0.72	0.708	5.312	0.248	24.8	6.4	1.7	8.9	3.1	7.7	6.72	1.61	11.51	0.945	99.82	40.7	112.7
826B	123	9.09	822	2.00	0.511	2830	2870	24.4	0.399	0.72	0.709	5.312	0.248	24.8	6.4	1.7	8.9	3.8	1.2	7.03	1.72	11	0.908	99.97	40.8	112.8
828A	121	11.5	824	2.00	0.454	2640	2860	24.38	0.397	0.714	0.712	6.223	0.249	34.3	6.3	1.5	8.6	2.8	8.7	5.91	1.97	12.64	1.07	99.79	41.4	132.1
829A	121	11.6	824	2.00	0.454	2630	2860	24.38	0.398	0.714	0.711	6.223	0.249	34.3	6.3	1.5	8.6	3.3	1.4	6.23	1.39	12.22	0.902	99.97	41.4	132.1
831A	150	7.56	821	2.00	0.448	2610	2870	24.4	0.374	0.664	0.658	5.87	0.23	35.2	8.4	2.1	11.7	4	4.4	5.51	1.63	12.88	0.961	99.89	31	95.1
832B	150	6.82	822	2.00	0.45	2620	2860	24.38	0.373	0.664	0.657	5.848	0.231	35.1	8.4	2.2	11.7	4.2	0.7	6.43	1.39	12.39	0.862	99.98	31	94.2

Table 4. (Continued.)

Rdg	P_{rb} psia	ΔP_{34} psi	T_3 °F	ϕ_{rb}	ϕ_{ov}	T_4‡ °F	T_{rb}‡ °F	M_{rb}‡ g/mol	W_d lbm/s	W_o lbm/s	W_i lbm/s	W_q lbm/s	W_f lbm/s	J‡	τ_{rb} ms	τ_{lb} ms	τ_{ov} ms	NO_x g/kg-f	CO g/kg-f	CO_2 %	UHC ppm	O_2 %	FARR	η %	$V_{ref,rb}$ ft/s	$V_{ref,lb}$ ft/s
834A	154	5.6	821	1.98	0.507	2810	2880	24.45	0.374	0.669	0.661	4.968	0.23	24.9	8.5	2.4	12	4.3	6.1	6.88	1.61	11.58	0.857	99.85	30.3	80.4
835B	150	5.95	824	2.03	0.518	2850	2840	24.3	0.375	0.668	0.661	4.959	0.235	25	8.4	2.3	11.7	5.3	1	6.73	1.5	11.22	0.904	99.97	31.2	83.3
838A	149	9.28	915	2.00	0.39	2500	2950	24.38	0.349	0.622	0.613	6.565	0.216	52.9	8.7	2	12	4.1	3.6	5.2	1.17	14.06	1.206	99.91	31.3	112.5
839B	151	9.08	916	2.00	0.39	2500	2960	24.39	0.35	0.625	0.613	6.565	0.216	52.7	8.8	2.1	12.1	4.8	0.8	5.09	0.82	13.79	0.908	99.98	30.9	111
841A	152	6.9	917	1.99	0.452	2720	2970	24.41	0.35	0.627	0.619	5.45	0.217	35.9	8.7	2.3	12.2	4.9	3.2	5.73	0.59	12.95	0.781	99.92	30.9	94
842B	153	6.22	918	1.99	0.451	2720	2970	24.42	0.351	0.627	0.618	5.446	0.216	35.8	8.8	2.3	12.3	5.6	0.5	5.99	0.7	12.54	0.877	99.99	30.7	92.7
844A	150	5.95	918	2.01	0.488	2840	2950	24.36	0.353	0.633	0.621	5.014	0.22	30	8.6	2.3	12	5.2	5.4	6.3	0.7	12.12	0.849	99.87	31.6	89
845B	153	5.52	916	2.02	0.487	2840	2940	24.34	0.348	0.627	0.614	4.984	0.218	30.3	8.9	2.4	12.5	5.7	0.7	7.07	0.58	11.65	0.893	99.98	30.6	85.8
847A	124	13.5	916	2.02	0.392	2510	2940	24.33	0.365	0.653	0.643	6.891	0.228	53	6.9	1.5	9.4	3.2	8.7	5.02	0.36	14.66	1.207	99.79	39.5	149.2
848B	125	13.2	913	2.00	0.388	2490	2960	24.4	0.368	0.662	0.652	6.977	0.228	52.9	6.8	1.5	9.3	3.8	1.8	4.93	0.36	14.58	0.868	99.96	39.5	150.8
849A	121	10.4	917	2.01	0.454	2730	2950	24.36	0.37	0.662	0.651	5.767	0.23	36.2	6.6	1.6	9.1	3.8	3.7	5.57	0.47	13.82	0.734	99.91	41	130.1
850B	120	9.81	919	2.02	0.456	2730	2940	24.33	0.368	0.659	0.649	5.749	0.23	36.3	6.6	1.6	9.1	4.1	0.7	5.89	0.24	13.21	0.82	99.98	41.2	131
852A	123	8.4	917	2.00	0.481	2820	2960	24.4	0.367	0.664	0.654	5.315	0.229	30.6	6.7	1.7	9.3	4.2	3.6	5.49	0.24	13.36	0.826	99.91	40.3	118.9
853B	122	9.18	916	2.00	0.483	2820	2960	24.39	0.369	0.665	0.653	5.307	0.23	30.4	6.7	1.7	9.2	4.6	0.6	6.06	0.47	12.62	0.784	99.98	40.7	119.9
855A	151	7.57	969	2.04	0.381	2520	2970	24.27	0.312	0.558	0.553	6.19	0.197	59.9	9.7	2.2	13.3	5.1	2.6	4.66	0.59	15.09	1.091	99.94	28.9	106.3
856B	151	7.92	972	1.98	0.371	2490	3040	24.47	0.314	0.561	0.555	6.207	0.193	59.4	9.5	2.2	13.2	5.3	0.6	5.03	0.13	14.66	0.846	99.99	29	106.8
858A	150	6.21	975	2.00	0.425	2680	3010	24.38	0.319	0.558	0.556	5.332	0.195	43.7	9.5	2.4	13.2	6.1	1.4	4.92	0.36	14.29	0.792	99.97	29.3	94.7
859B	149	6.9	969	1.99	0.422	2670	3020	24.41	0.316	0.559	0.557	5.329	0.194	43.7	9.4	2.3	13.1	6.1	0.3	5.22	0.47	13.87	0.798	99.99	29.4	95.8
861A	151	5.17	971	2.01	0.465	2820	3000	24.36	0.313	0.555	0.554	4.719	0.194	34.8	9.6	2.5	13.5	6.5	1.3	5.45	0.82	13.55	0.769	99.97	28.8	84.6
862B	150	5.79	972	1.99	0.461	2810	3030	24.44	0.318	0.559	0.559	4.75	0.194	34.6	9.4	2.5	13.3	6.7	0.4	5.82	0.13	13.03	0.809	99.99	29.3	85.9
864A	121	6.73	972	2.02	0.469	2830	2990	24.33	0.316	0.558	0.557	4.726	0.197	34.5	7.7	2	10.7	5.1	2.3	5.38	0.24	13.66	0.847	99.95	36.3	109
865B	122	6.55	971	2.01	0.467	2820	3000	24.35	0.317	0.56	0.56	4.757	0.197	34.7	7.7	2	10.7	5.4	0.5	5.83	0.47	13.03	0.789	99.99	36.1	108.6
866A	121	8.41	969	2.02	0.429	2690	2990	24.32	0.315	0.555	0.556	5.293	0.196	43.5	7.7	1.9	10.6	4.9	2.5	4.98	0.59	14.28	0.928	99.94	36.1	119.7
867B	120	8.16	975	2.02	0.43	2700	2990	24.31	0.315	0.557	0.556	5.292	0.196	43.4	7.6	1.8	10.5	4.9	0.5	5.38	0.47	13.85	0.792	99.99	36.6	120.2
869A	81.2	14.2	973	2.02	0.429	2700	2990	24.33	0.315	0.559	0.558	5.298	0.196	43.3	5.1	1.1	6.9	2.1	12	4.9	0.36	14.3	0.85	99.72	54.1	201.9
870B	79.9	14.7	973	2.08	0.441	2740	2920	24.14	0.312	0.55	0.551	5.234	0.2	43.7	5.2	1.1	6.9	2.3	2.1	5.32	0.59	13.66	0.765	99.95	54.4	205.3
875A	153	4.87	590	1.90	0.499	2550	2750	24.75	0.372	0.659	0.65	4.717	0.217	20	9.1	2.7	13	3.2	17.3	6.56	2.98	12.18	0.732	99.59	24.5	63.5
876B	149	5.59	590	2.01	0.523	2630	2620	24.36	0.355	0.626	0.619	4.538	0.218	20.7	9.5	2.6	13.4	3.9	0.9	6.91	0.81	11.39	0.851	99.98	24.1	62.6
878A	152	4.54	591	2.02	0.575	2800	2610	24.31	0.342	0.625	0.623	4.013	0.219	16.5	9.8	2.8	13.8	3.3	27.3	6.75	4.12	11.6	0.823	99.35	23.6	55.7
879B	154	3.23	590	2.01	0.563	2760	2620	24.37	0.343	0.621	0.623	4.073	0.217	17	9.9	2.9	14	4.5	1.5	7.61	0.24	10.48	0.827	99.97	23.2	55.1
883A	81.4	9.51	592	2.02	0.571	2790	2610	24.33	0.371	0.672	0.658	4.309	0.234	16.6	4.9	1.3	6.7	1.3	68.6	6.45	6.76	11.73	0.907	98.38	47.1	122.6
884B	79.6	10.9	595	2.02	0.572	2800	2620	24.33	0.373	0.668	0.656	4.293	0.233	16.6	4.8	1.2	6.5	1.7	9.4	7.33	0.12	10.51	0.798	99.78	48.2	128.1
886A	80.4	12.9	593	2.03	0.526	2650	2600	24.29	0.37	0.668	0.655	4.836	0.234	21.2	4.9	1.2	6.6	1.2	60.8	6.01	2.77	12.34	0.967	98.56	47.5	142.3
887B	81	13	596	2.03	0.526	2650	2610	24.3	0.368	0.663	0.651	4.808	0.232	21.3	4.9	1.2	6.6	1.6	6.1	6.73	0.47	11.41	0.809	99.85	47	140.6
891A	145	7.21	1025	2.02	0.37	2540	3050	24.34	0.307	0.529	0.528	6.075	0.187	63.8	9.5	2.2	13.1	6.6	2	4.6	3.51	13.29	1.263	99.94	29.9	112.5
892A	144	6.96	1036	2.02	0.371	2560	3050	24.32	0.306	0.528	0.527	6.049	0.187	64.4	9.4	2.1	13	6.6	2	4.59	1.53	13.29	0.912	99.95	30.3	114.1
896A	145	6.18	1057	2.00	0.371	2580	3100	24.4	0.304	0.54	0.528	6.024	0.186	63.1	9.3	2.2	12.9	7.9	2.5	4.14	1.48	13.64	0.912	99.94	30.7	113.7
897B	145	5.58	1057	2.00	0.371	2580	3100	24.39	0.303	0.54	0.528	6.024	0.186	63.3	9.3	2.2	13	7.9	0.5	4.56	1.42	13.39	0.836	99.98	30.7	112.8
899A	145	6.62	1067	2.03	0.459	2890	3070	24.27	0.36	0.655	0.656	5.739	0.231	38.6	7.7	1.9	10.7	8.4	2.6	5.54	0.94	12.21	0.73	99.94	37.7	114.3
900B	147	6.8	1067	2.04	0.459	2900	3070	24.27	0.361	0.655	0.654	5.735	0.231	38.9	7.8	2	10.8	8.6	0.6	5.68	0.82	12.2	0.874	99.98	37.2	113.7
901A	151	7.57	1047	1.98	0.368	2560	3110	24.46	0.34	0.612	0.6	6.801	0.209	62.5	8.6	2	11.9	7.1	3.4	4.45	0.71	14.07	1.108	99.92	33.1	123.1

Table 4. (Concluded.)

Rdg	P_{rb} psia	ΔP_{34} psi	T_3 °F	ϕ_{rb}	ϕ_{ov}	T_4‡ °F	T_{rb}‡ °F	M_{rb}‡ g/mol	W_d lbm/s	W_o lbm/s	W_i lbm/s	W_q lbm/s	W_f lbm/s	J‡	τ_{rb} ms	τ_{lb} ms	τ_{ov} ms	NO_x g/kg-f	CO g/kg-f	CO_2 %	UHC ppm	O_2 %	FARR	η %	$V_{ref,rb}$ ft/s	$V_{ref,lb}$ ft/s
902B	152	7.67	1046	2.00	0.369	2560	3090	24.41	0.34	0.612	0.601	6.845	0.211	63.4	8.7	2	12	7.4	0.6	4.57	0.94	13.96	0.864	99.98	32.9	123.8
903A	150	9.17	1039	2.01	0.405	2680	3080	24.38	0.369	0.662	0.663	6.695	0.231	50.7	7.9	1.9	10.9	7.9	2.6	5.26	0.71	13.29	0.806	99.94	36.2	125.6
904B	151	8.1	1039	2.01	0.406	2680	3070	24.36	0.368	0.662	0.661	6.675	0.231	50.6	7.9	1.9	11	7.9	0.5	5.31	0.71	13.19	0.909	99.99	35.9	123.5
905A	152	8.82	1040	2.01	0.452	2840	3070	24.37	0.411	0.74	0.732	6.478	0.257	38.5	7.2	1.8	10	8.5	2	5.44	0.82	12.89	0.825	99.95	39.8	123.4
906A	153	8.6	1043	2.00	0.45	2840	3090	24.4	0.409	0.742	0.732	6.471	0.256	38.3	7.2	1.8	10	8.6	0.5	5.91	0.59	12.45	0.854	99.99	39.6	121.7
907A	150	12	1019	2.01	0.369	2530	3050	24.36	0.392	0.712	0.7	8.017	0.247	63.3	7.4	1.7	10.2	8.1	5	4.34	0.83	14.47	1.116	99.88	38.1	146.6
908B	153	12.1	1011	2.00	0.367	2520	3060	24.4	0.395	0.714	0.702	8.048	0.246	63.4	7.6	1.7	10.4	8.1	0.9	4.64	0.48	14.14	0.838	99.98	37.2	144.7
909C	153	11.5	1009	1.99	0.364	2500	3060	24.42	0.391	0.715	0.702	8.084	0.245	63.7	7.6	1.7	10.4	8.2	0.3	4.75	0.59	14.03	0.898	99.99	37.1	144.6
911B	152	11	1003	1.99	0.401	2630	3060	24.42	0.43	0.776	0.773	7.852	0.268	50.3	6.9	1.6	9.5	9	0.4	4.96	0.94	13.71	0.832	99.99	40.7	143.5
912A	151	11	1003	1.99	0.401	2630	3050	24.42	0.428	0.776	0.773	7.852	0.268	50.3	6.8	1.6	9.5	8.6	4.1	4.54	0.59	14.35	0.869	99.9	41	143.4
913A	152	10.4	1006	1.99	0.449	2800	3060	24.44	0.479	0.869	0.859	7.568	0.298	37.5	6.2	1.6	8.6	8.5	2.9	4.92	0.48	13.72	0.711	99.93	45.5	141.7
914B	152	10.2	1005	2.00	0.45	2800	3050	24.4	0.477	0.87	0.858	7.591	0.299	37.9	6.2	1.5	8.6	8.8	0.4	5.46	0.82	12.89	0.771	99.99	45.5	142
916A	123	9.29	1032	2.00	0.447	2820	3070	24.39	0.409	0.73	0.727	6.487	0.254	39.1	5.9	1.4	8.1	7.7	3.7	4.93	0.71	13.62	0.861	99.91	48.4	154
917B	124	10.4	1040	2.00	0.447	2830	3080	24.39	0.409	0.729	0.727	6.478	0.254	39.2	5.9	1.4	8.1	8.5	0.4	5.45	0.24	12.98	0.779	99.99	48.3	154.8
918A	151	6.68	1080	2.02	0.454	2890	3110	24.34	1.105	0.394	0.184	5.782	0.231	38.4	7.9	2	11	13.2	2.8	5.42	0.82	12.89	0.843	99.93	36.7	110.8
919B	151	6.55	1080	2.02	0.455	2900	3100	24.33	1.103	0.393	0.184	5.768	0.231	38.4	7.9	2	11	13.7	0.7	5.99	0.59	12.06	0.842	99.98	36.7	111.3
921A	125	2.96	591	2.00	0.526	2640	2630	24.38	0.42	0.75	0.76	5.428	0.263	20.4	6.6	1.9	9.3	3.9	4.2	5.96	30.45	11.6	0.805	99.84	34.7	88.1
922B	125	2.42	593	2.00	0.524	2640	2640	24.4	0.419	0.752	0.755	5.423	0.262	20.4	6.6	1.9	9.3	4.3	0.8	6.15	17.88	11.39	0.825	99.95	34.7	88.1
923A	117	0.71	592	1.79	0.517	2610	2890	25.19	0.468	0.845	0.823	5.266	0.26	15.3	5.4	1.8	7.9	3.8	3.3	6.22	6.54	11.28	0.858	99.91	40.6	93.2
924B	116	0.34	592	1.80	0.519	2620	2880	25.17	0.467	0.842	0.823	5.264	0.261	15.4	5.3	1.8	7.9	4.2	0.6	6.43	4.13	10.88	0.867	99.98	40.9	94
925A	120	4.8	591	1.59	0.516	2610	3160	26.08	0.526	0.939	0.93	5.007	0.26	10.8	4.8	1.8	7.2	3.4	2.6	6.04	3.57	11.68	0.903	99.93	43.8	94.7
926B	121	4.68	591	1.60	0.517	2610	3150	26.06	0.526	0.94	0.926	5.004	0.26	10.8	4.8	1.8	7.3	4	0.5	6.4	2.65	11.17	0.839	99.98	43.4	93.9
927A	122	4.86	592	1.50	0.527	2650	3300	26.53	0.569	1.021	1	4.774	0.264	8.3	4.4	1.8	6.8	3.4	2.2	6.01	1.73	12.06	0.87	99.94	46.4	92
928B	122	4.65	592	1.50	0.526	2640	3300	26.54	0.57	1.021	1.002	4.782	0.264	8.3	4.4	1.8	6.8	3.9	0.5	6.45	1.73	11.44	0.807	99.98	46.4	92.8
930A	122	4.93	591	2.18	0.517	2610	2420	23.81	0.382	0.691	0.679	5.645	0.26	27.5	7.4	1.8	10.1	3.7	5.2	5.9	1.62	12.26	0.879	99.87	32.7	93.2
931B	122	4.83	590	2.18	0.519	2620	2420	23.81	0.384	0.691	0.678	5.626	0.26	27.3	7.3	1.8	10.1	4.5	1.1	6.24	1.27	11.66	0.802	99.97	32.6	92.9
932A	120	4.08	819	2.01	0.457	2640	2850	24.35	0.332	0.592	0.592	5.155	0.208	34	7.5	1.9	10.5	5.8	2.5	4.89	1.29	13.63	0.966	99.94	34.6	103.5
933B	120	3.29	821	2.00	0.455	2640	2860	24.39	0.331	0.592	0.594	5.151	0.206	33.9	7.5	2	10.5	6.8	0.4	5.33	1.05	13	0.762	99.99	34.6	102.7
934A	121	4.25	822	1.81	0.453	2630	3110	25.14	0.368	0.661	0.653	5.012	0.206	25.7	6.6	2	9.6	5.4	2.1	4.98	1.06	13.43	0.833	99.95	37.7	103.1
935B	120	4.36	821	1.80	0.452	2630	3110	25.17	0.368	0.661	0.656	5.016	0.206	25.6	6.5	2	9.5	5.7	0.4	5.28	1.05	13.01	0.784	99.99	38	103.1
936A	121	4.11	825	1.60	0.45	2620	3380	26.05	0.408	0.738	0.728	4.787	0.204	18.6	5.8	2	8.6	4.5	1.8	5.17	0.82	13.12	0.833	99.96	41.5	102.7
937B	122	4.12	826	1.59	0.448	2610	3400	26.09	0.409	0.739	0.731	4.807	0.204	18.6	5.8	2	8.7	5	0.3	5.45	0.71	12.79	0.823	99.99	41.3	102.3
938A	147	6.04	829	2.01	0.511	2830	2860	24.37	0.496	0.884	0.876	6.61	0.308	25.2	6.2	1.7	8.7	6.2	1.8	5.29	1.28	13.01	0.756	99.96	42.3	113.5
939B	147	6.01	826	2.00	0.508	2820	2870	24.41	0.496	0.885	0.88	6.615	0.307	25.1	6.1	1.7	8.6	7.1	0.4	5.73	1.51	12.38	0.739	99.99	42.3	113.4
940A	151	6.99	827	2.00	0.458	2650	2880	24.41	0.496	0.883	0.882	7.599	0.307	33.2	6.3	1.6	8.8	6.7	3.4	4.59	0.71	14.15	0.887	99.92	41.2	123.5
942B	152	6.94	826	1.99	0.457	2650	2880	24.42	0.496	0.887	0.883	7.602	0.307	33.1	6.3	1.6	8.9	7.7	0.4	5.43	0.71	12.99	0.709	99.99	41	122.6
945A	125	3.25	834	1.59	0.592	3100	3410	26.08	0.517	0.91	0.908	3.945	0.253	8.1	4.8	1.9	7.3	5.9	3.2	7.32	0.69	10.04	0.645	99.92	50.5	93.4
946B	126	3.12	829	1.59	0.591	3090	3400	26.1	0.518	0.912	0.912	3.96	0.253	8.1	4.8	1.9	7.4	7.5	0.8	7.24	0.58	10.24	0.878	99.98	50	92.6

‡Estimated.

Table 5. Selected RQL Combustor Smoke Number Performance Data

Rdg	P_{rb} psia	ΔP_{34} psi	T_3 °F	ϕ_{rb}	ϕ_{ov}	T_4 °F	T_{rb} °F	M_{rb} g/mol	W_d lbm/s	W_o lbm/s	W_i lbm/s	W_q lbm/s	W_f lbm/s	J	τ_{rb} ms	τ_{lb} ms	τ_{ov} ms	NO_x g/kg-f	CO g/kg-f	CO_2 %	UHC ppm	O_2 %	Smoke number	η %	$V_{ref,rb}$ ft/s	$V_{ref,lb}$ ft/s
714A	83	0.56	828	2.01	0.512	2830	2860	24.37	0.425	0.21	0.083	2.099	0.098	67.8	11	3.1	16.5		6.5	6.91	53.88	10.66	40	99.75	23.7	61.2
717C	80	?	828	2.00	0.511	2830	2880	24.41	0.427	0.21	0.083	2.093	0.098	67.9	10.5	3.1	15.9	8	0.6	7.29	10.6	10.76	7	99.97	24.7	61.8
719B	80	?	829	2.00	0.514	2840	2870	24.38	0.427	0.209	0.084	2.087	0.098	67.5	10.5	3.1	15.9	7.3	7.2	7.56	8.04	10.41	6.9	99.82	24.8	61.1
730C	80	?	824	1.99	0.446	2610	2880	24.43	0.391	0.242	0.268	3.116	0.122	95.7	8.4	2.3	12.7	4.3	0.6	6.3	5.39	12.66	3.6	99.98	30.8	89.6
732B	80	0.94	826	2.01	0.452	2630	2850	24.35	0.388	0.24	0.267	3.086	0.122	95.7	8.5	2.3	12.7	4	1.4	5.49	5.1	13.51	4.1	99.96	30.7	90.2
741C	79	5.11	827	2.00	0.449	2620	2870	24.40	0.521	0.327	0.355	4.151	0.163	95.1	6.2	1.6	9.1	0.3	0.6	6.37	3.56	12.66	0	99.98	42.1	130.7
756A	81	4.53	828	1.99	0.402	2460	2880	24.41	0.556	0.251	0.104	3.611	0.124	46	8.3	2	11.6	0	?	0	0	0	20		31.1	106.3
757B	80	3.49	827	2.00	0.403	2460	2870	24.41	0.559	0.251	0.104	3.618	0.124	46	8.3	2	11.6	0.9	?	0	0	0	9.8		31.4	106.1
758C	81	3.34	830	1.97	0.401	2460	2910	24.50	0.566	0.255	0.105	3.622	0.124	44.9	8.2	2	11.5	1	?	0	0	0	7		31.6	105.9
759A	121	11.90	826	2.02	0.414	2500	2850	24.33	0.779	0.489	0.551	7.045	0.25	44	6.3	1.4	8.6	2.6	9.3	0	0		16.3	99.94	41.4	146.6
760B	121	11.80	826	2.00	0.411	2490	2870	24.39	0.779	0.49	0.551	7.045	0.248	43.9	6.3	1.5	8.6	16.3	2.1				10.7		41.4	145.3
762C	120	11.40	832	2.03	0.416	2510	2840	24.29	0.768	0.484	0.545	6.977	0.248	44.4	6.3	1.5	8.7	3.6	0.5				7.3		41.5	145.8
894C	148	6.74	1044	2.01	0.357	2510	3080	24.36	0.306	0.525	0.526	6.282	0.185	69.5	9.7	2.2	13.4			4.36	1.88	13.61	0.1	99.94	29.5	113.7
899C	145	6.62	1067	2.03	0.459	2890	3070	24.27	0.36	0.655	0.656	5.739	0.231	38.6	7.7	1.9	10.7			5.54	0.94	12.21	2.6	99.94	37.7	114.3
902C	152	7.67	1046	2.00	0.369	2560	3090	24.41	0.34	0.612	0.601	6.845	0.211	63.4	8.7	2	12			4.57	0.94	13.96	1.8	99.98	32.9	123.8

Editor's note: There was no mention in the original draft concerning the quick-mix section geometry during the smoke number tests. However, since these readings preceeded chronologically and partially overlapped the data in Table 4, the geoetry is assumed to be the same as that in Table 4.

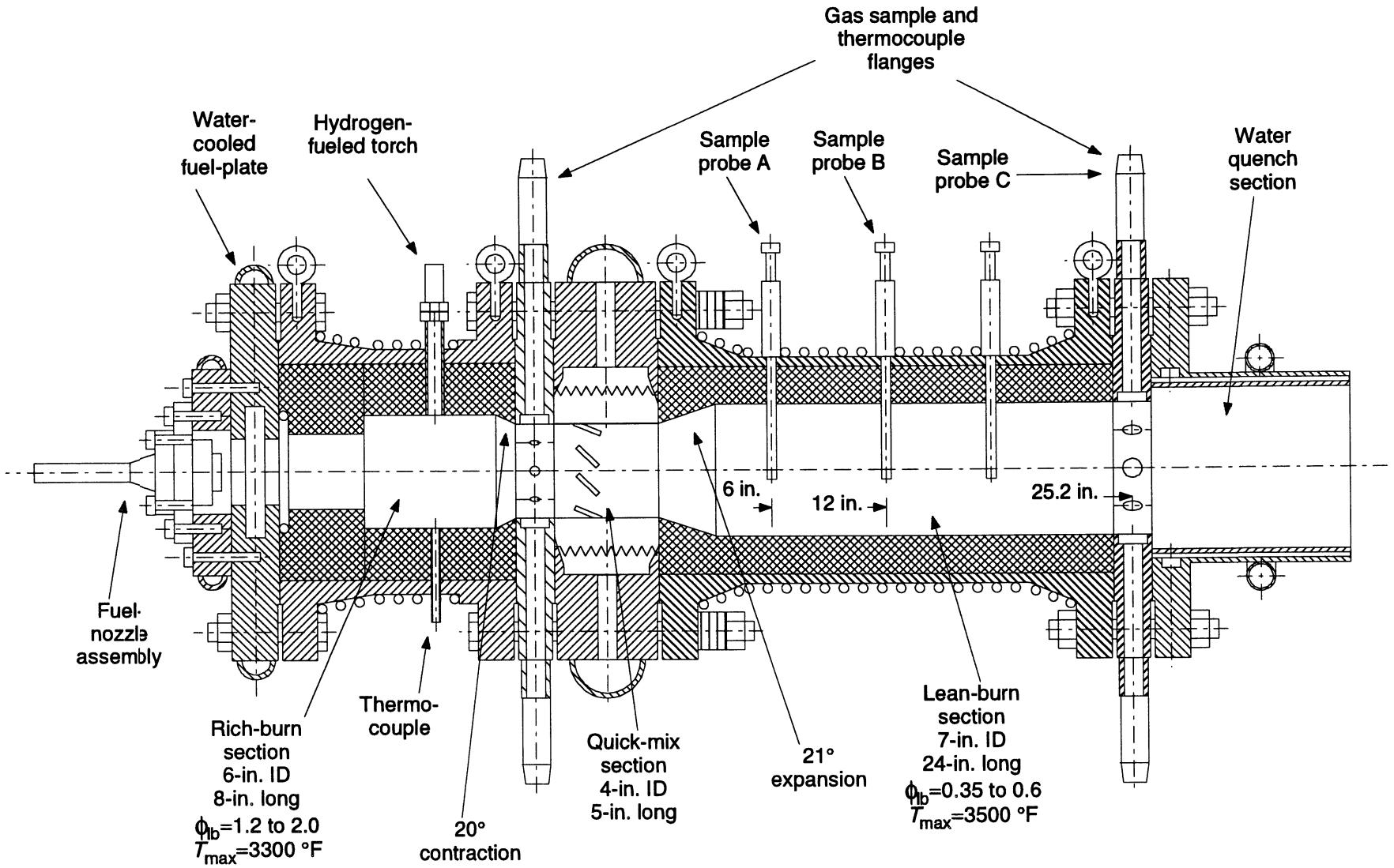

Figure 1. Cut-away drawing of RQL combustor test rig with instrumentation locations.

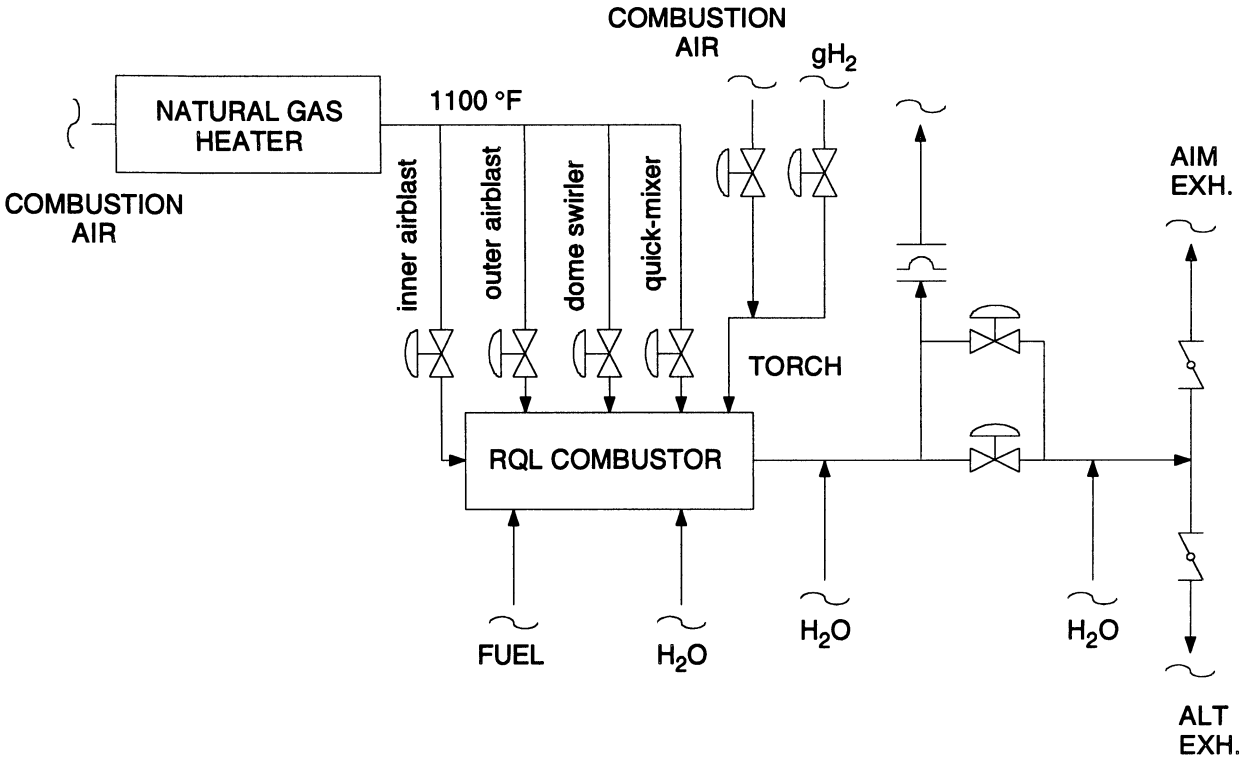

Figure 2. Schematic diagram of RQL rig flow controls.

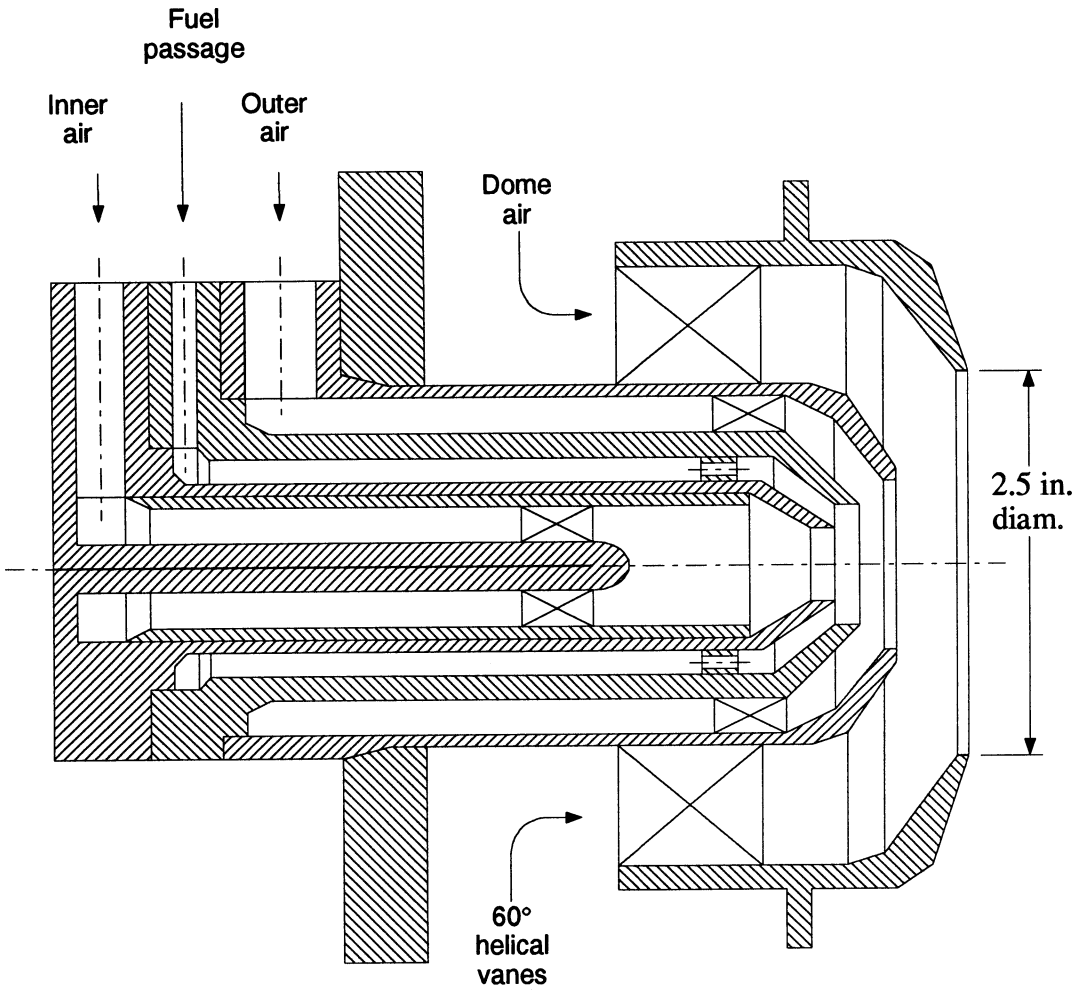

Figure 3. Conceptual sketch of Parker Airblast Low NO_x Nozzle (Phase I).

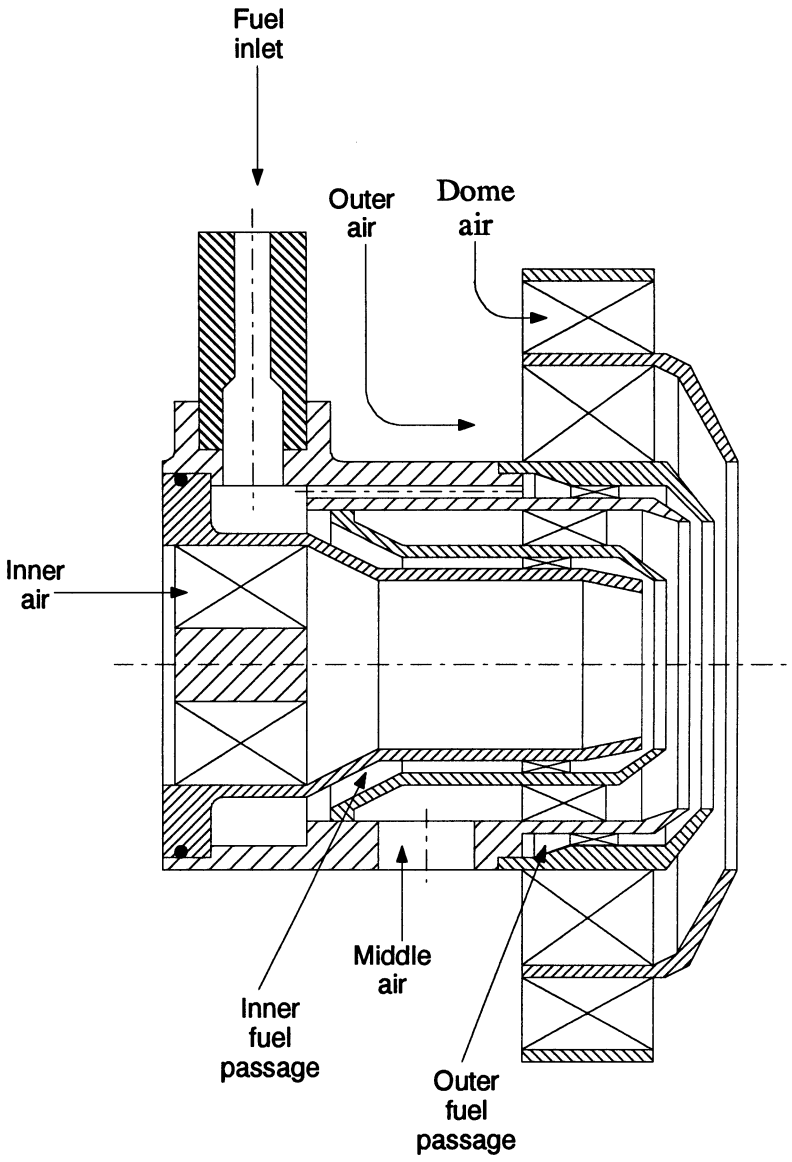

Figure 4. Conceptual sketch of Textron fuel nozzle cross-section.

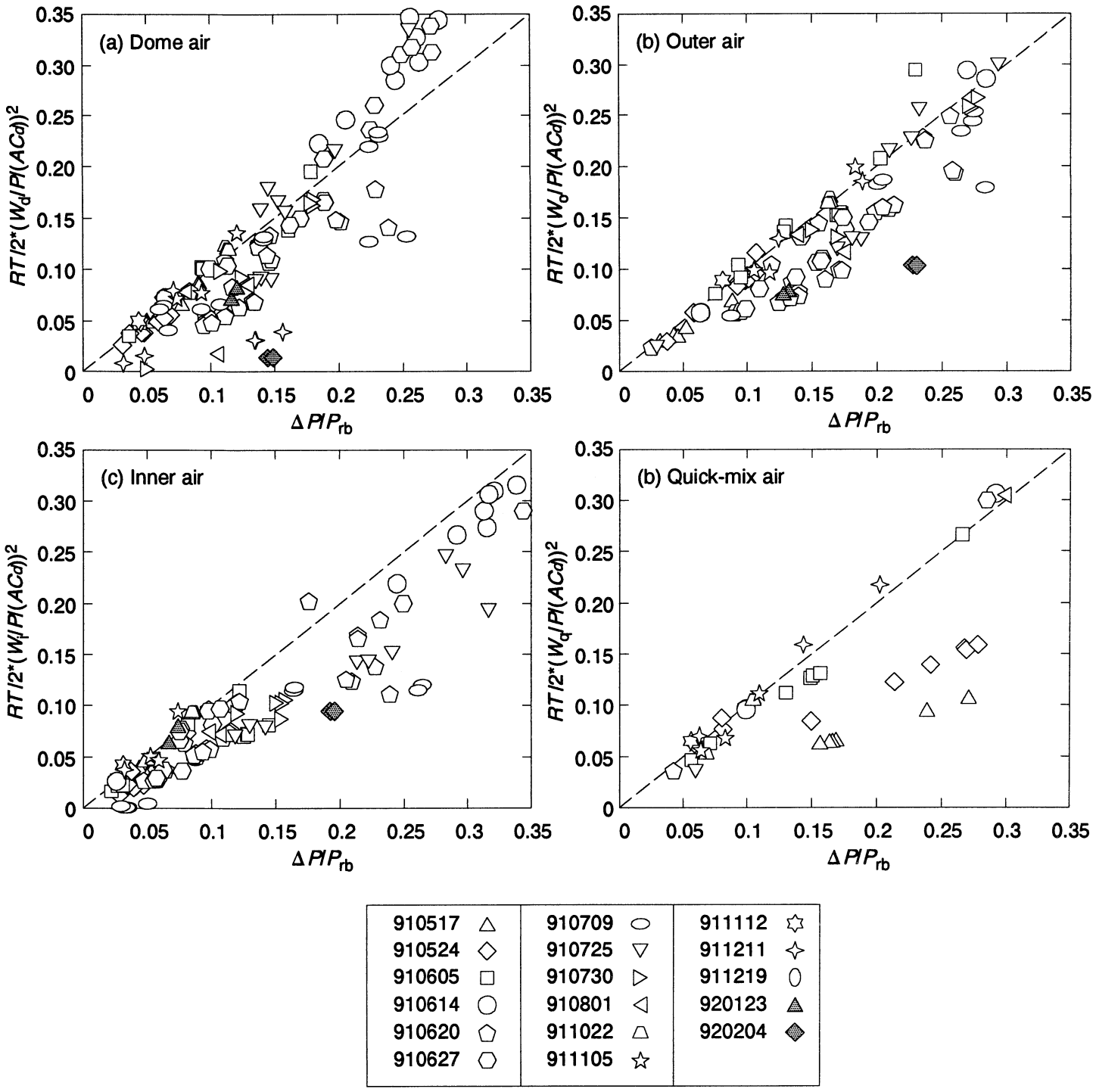

Figure 5. RQL combustor non-burning nozzle flow pressure drop fractions versus respective flow parameters. Test dates are shown with corresponding symbols. The shaded symbols were for Textron nozzle; the rest were done with the Parker nozzle. The effective discharge areas are listed in Table 1.

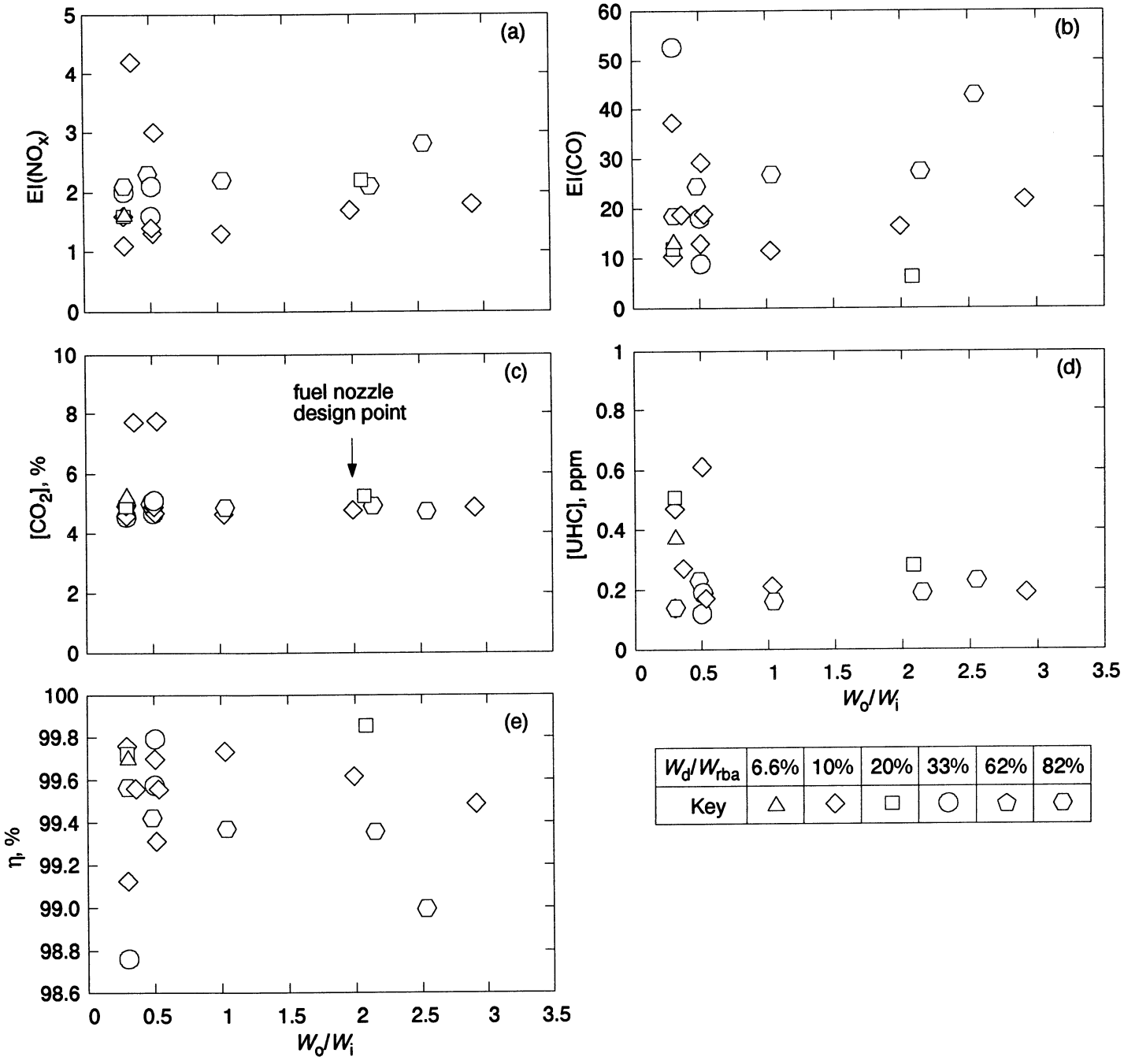

Figure 6. Effect of Parker nozzle individual air circuit on emissions measured by probe A.

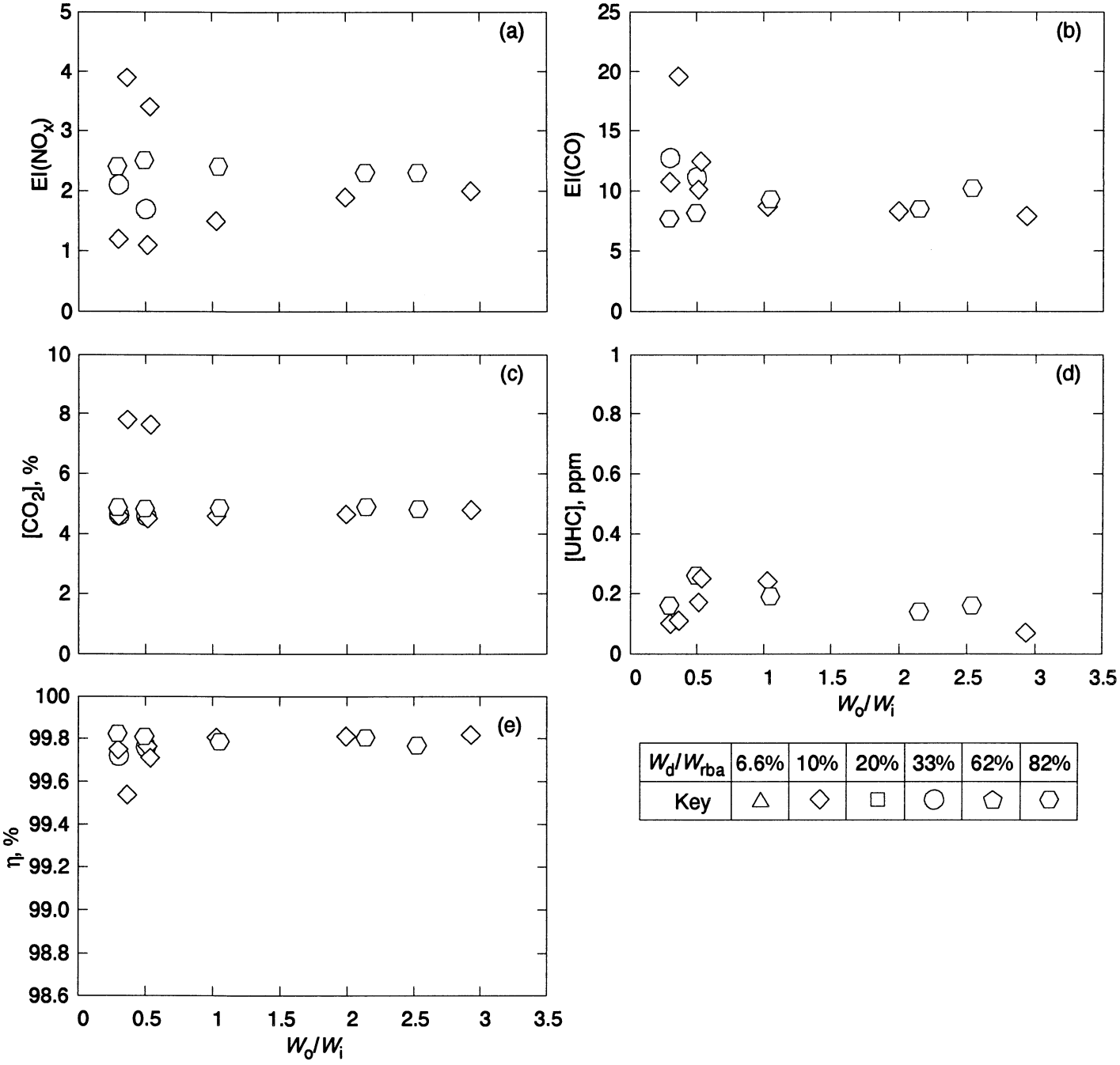

Figure 7. Effect of Parker nozzle individual air circuit on emissions measured by probe B.

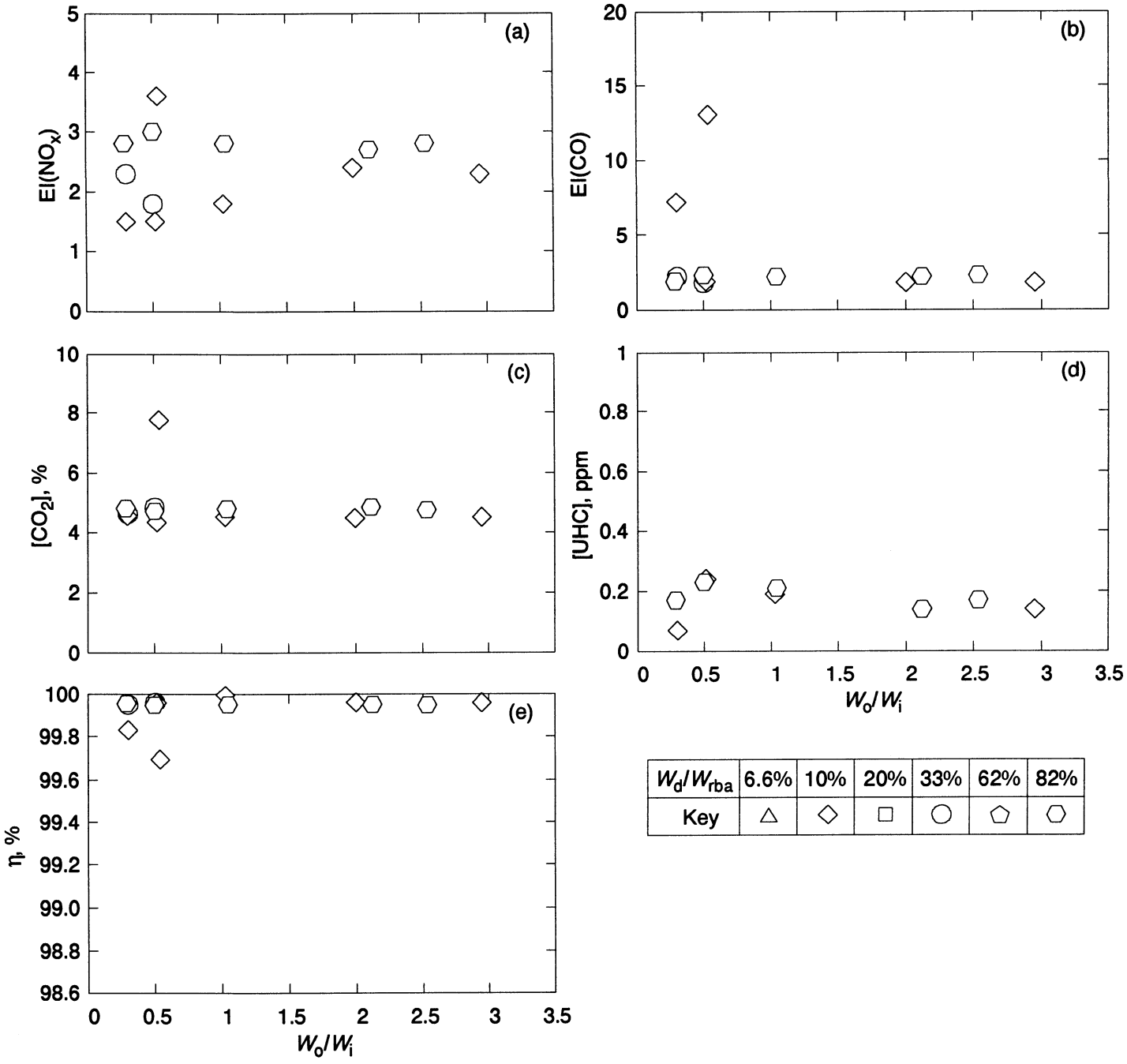

Figure 8. Effect of Parker nozzle individual air circuit on emissions measured by probe C.

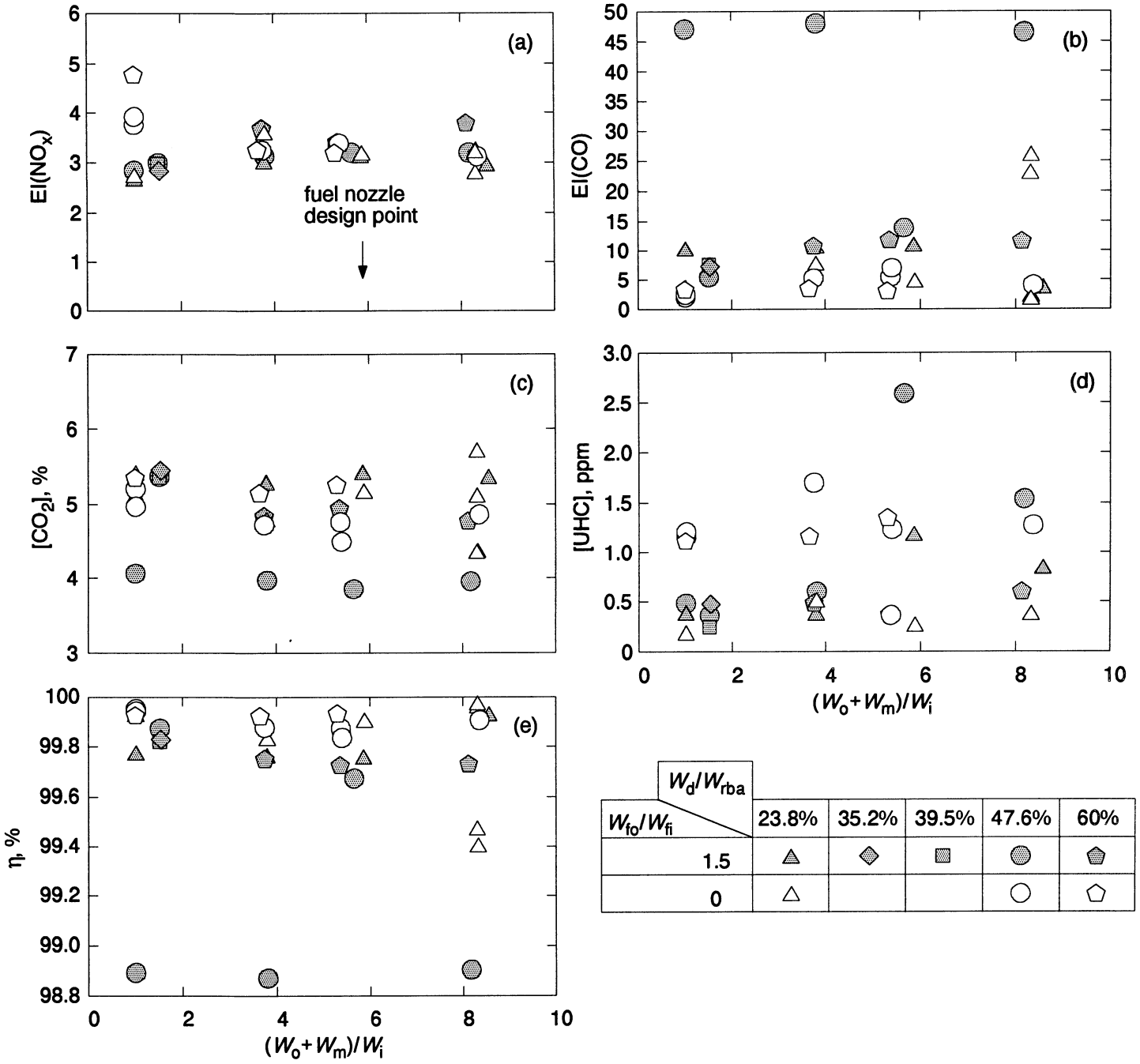

Figure 9. Effect of Textron nozzle air and fuel circuits on emissions measured by probe A.

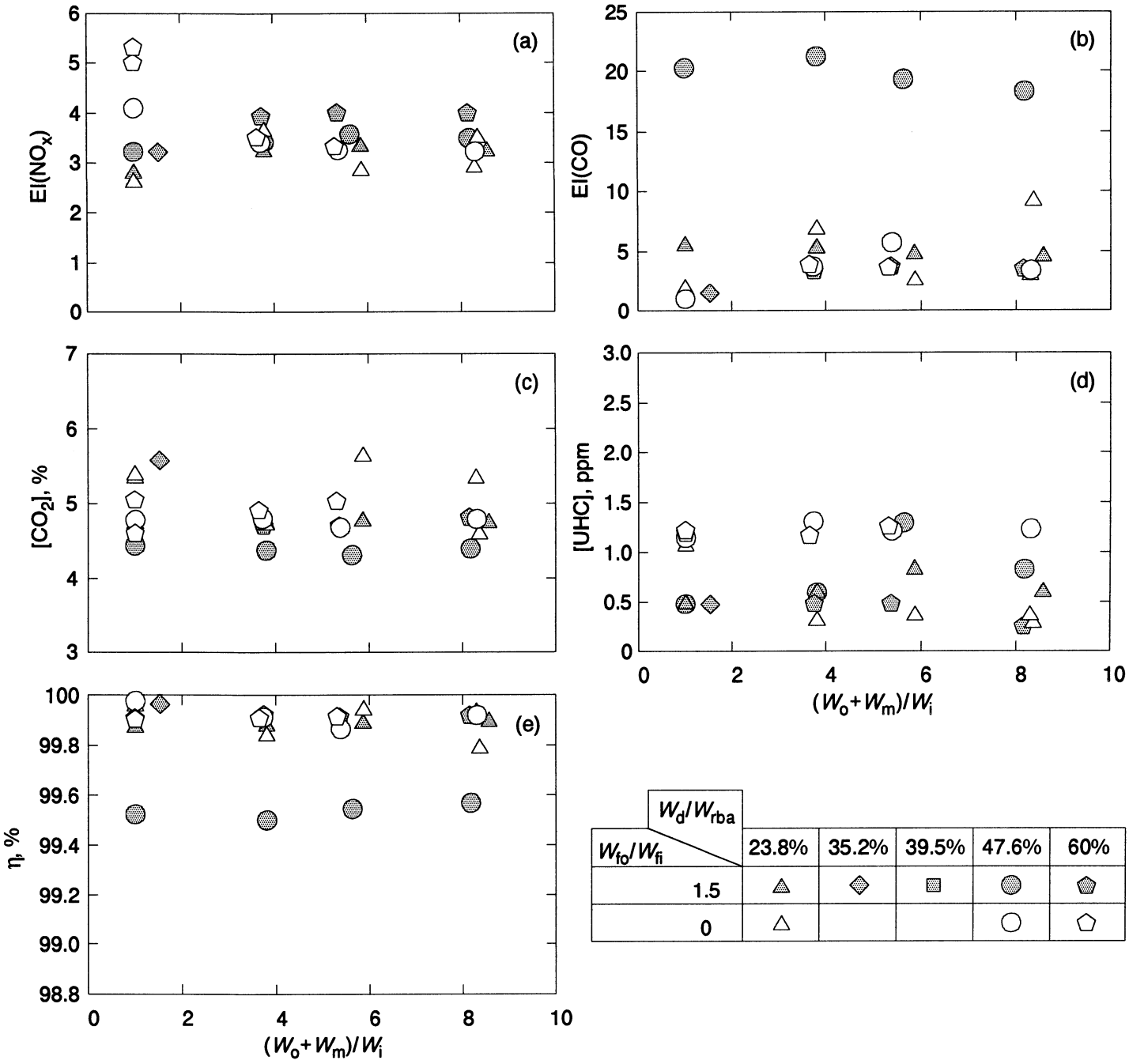

Figure 10. Effect of Textron nozzle air and fuel circuits on emissions measured by probe B.

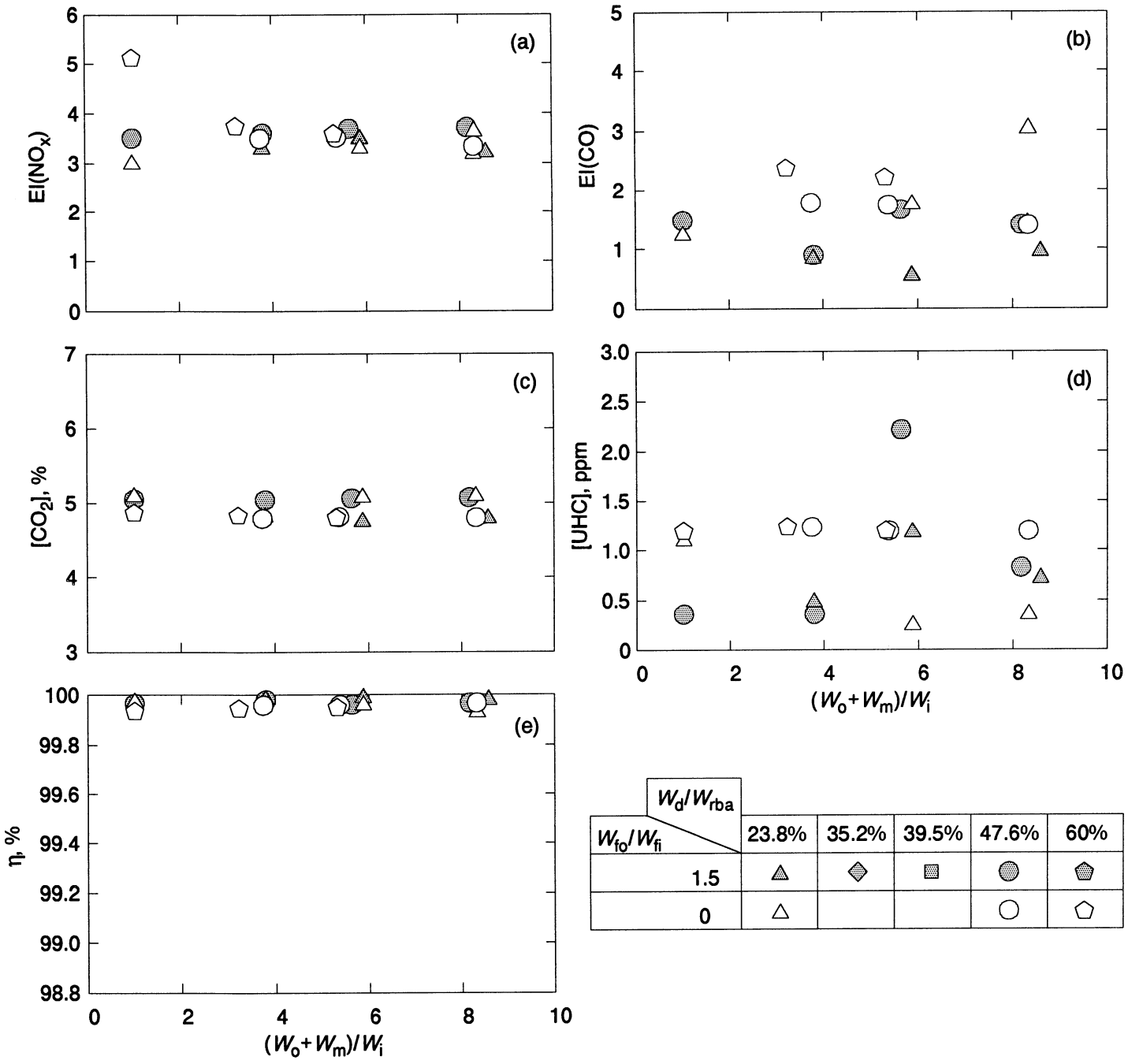

Figure 11. Effect of Textron nozzle air and fuel circuits on emissions measured by probe C.

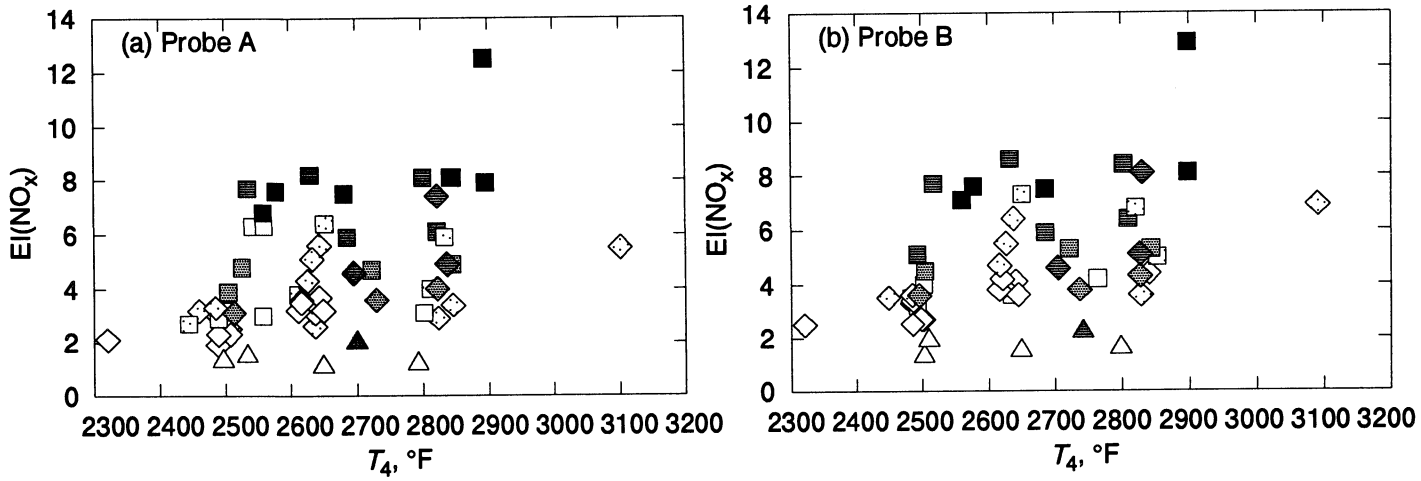

P_{rb} \ T_3	600	840	940	1000	1100
80	△	△	▲	▲	▲
120	◇	◇	◆	◆	◆
150	□	□	■	■	■

Figure 12. Variation of EI(NO_x) with T_4.

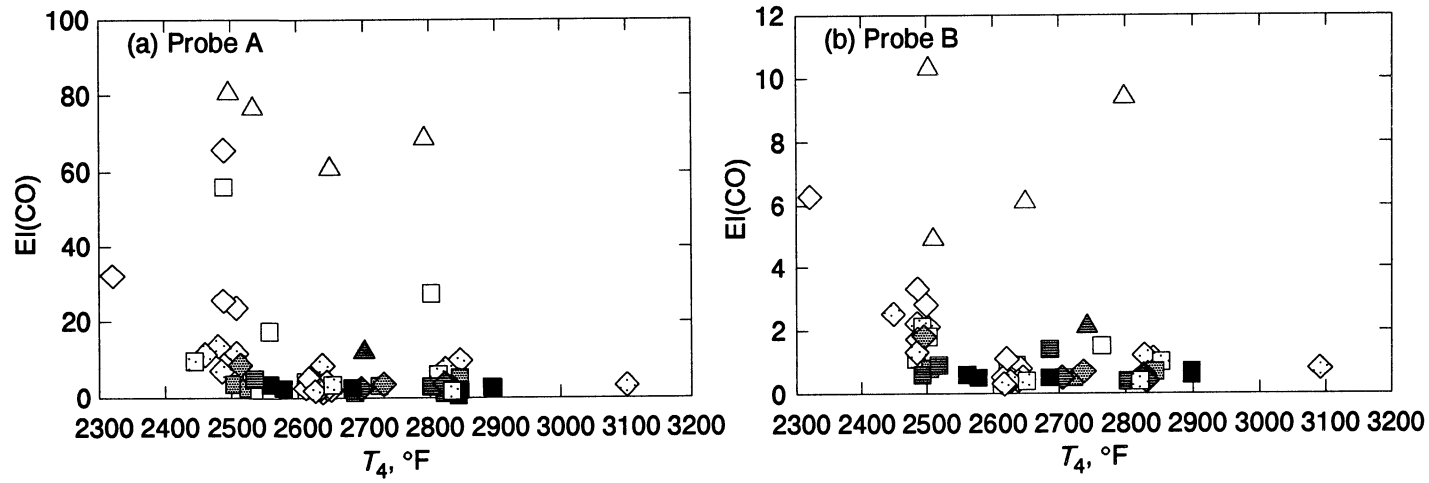

P_{rb} \ T_3	600	840	940	1000	1100
80	△	△	▲	▲	▲
120	◇	◇	◆	◆	◆
150	□	□	■	■	■

Figure 13. Variation of EI(CO) with T_4.

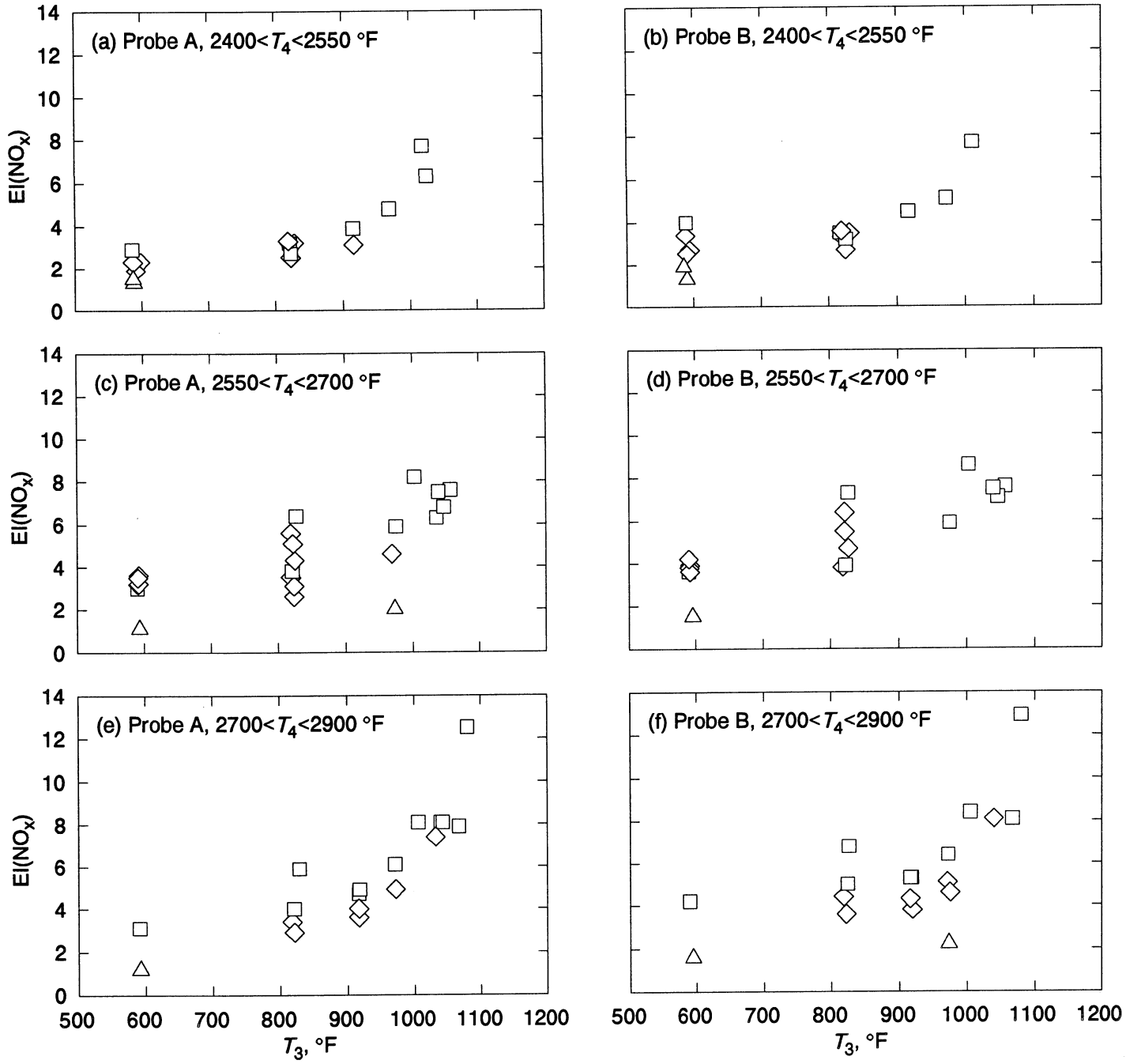

P_{rb}	80	120	150
Key	△	◇	□

Figure 14. Variation of EI(NO_x) with T_3.

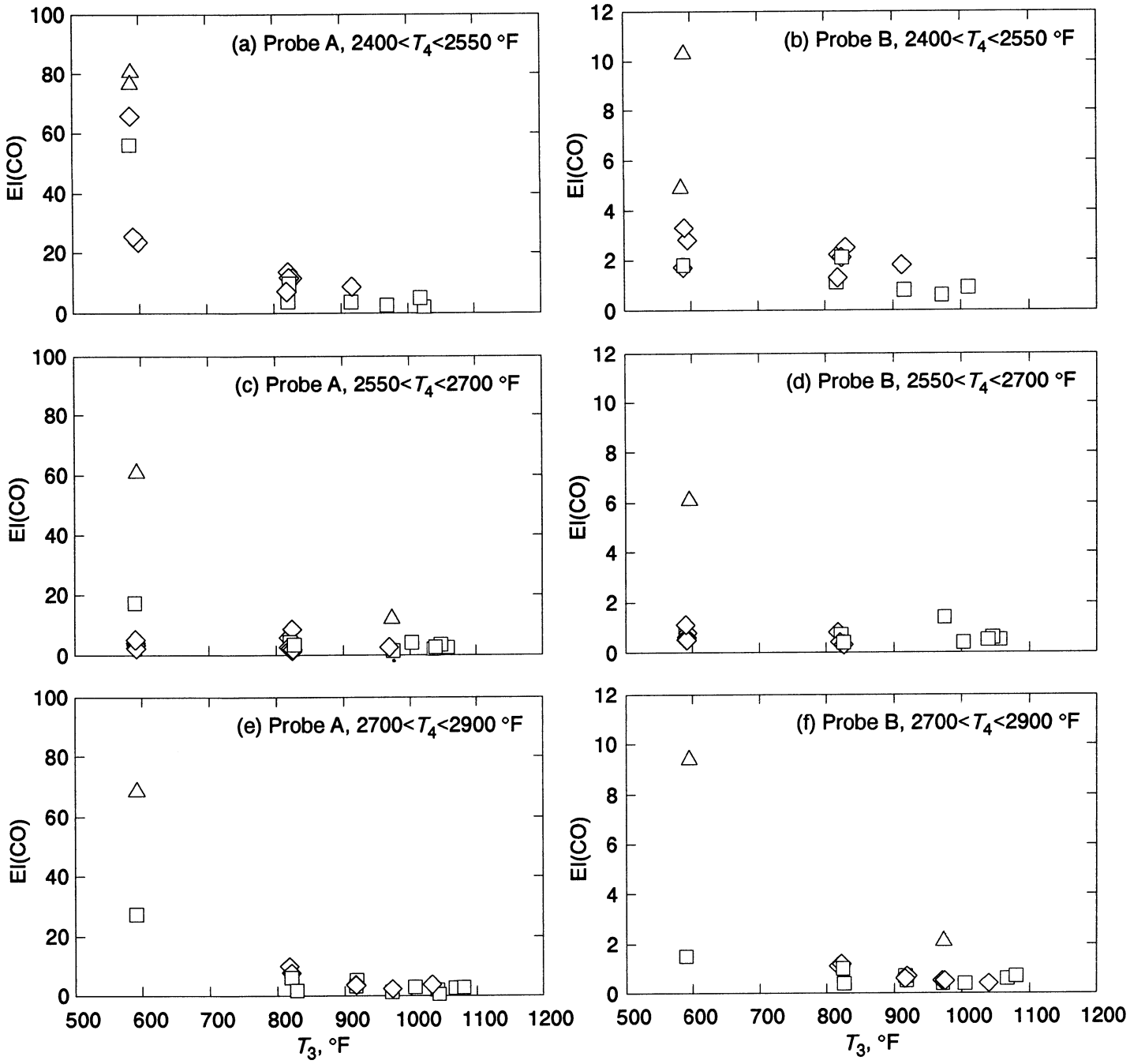

P_{rb}	80	120	150
Key	△	◇	□

Figure 15. Variation of EI(CO) with T_3.

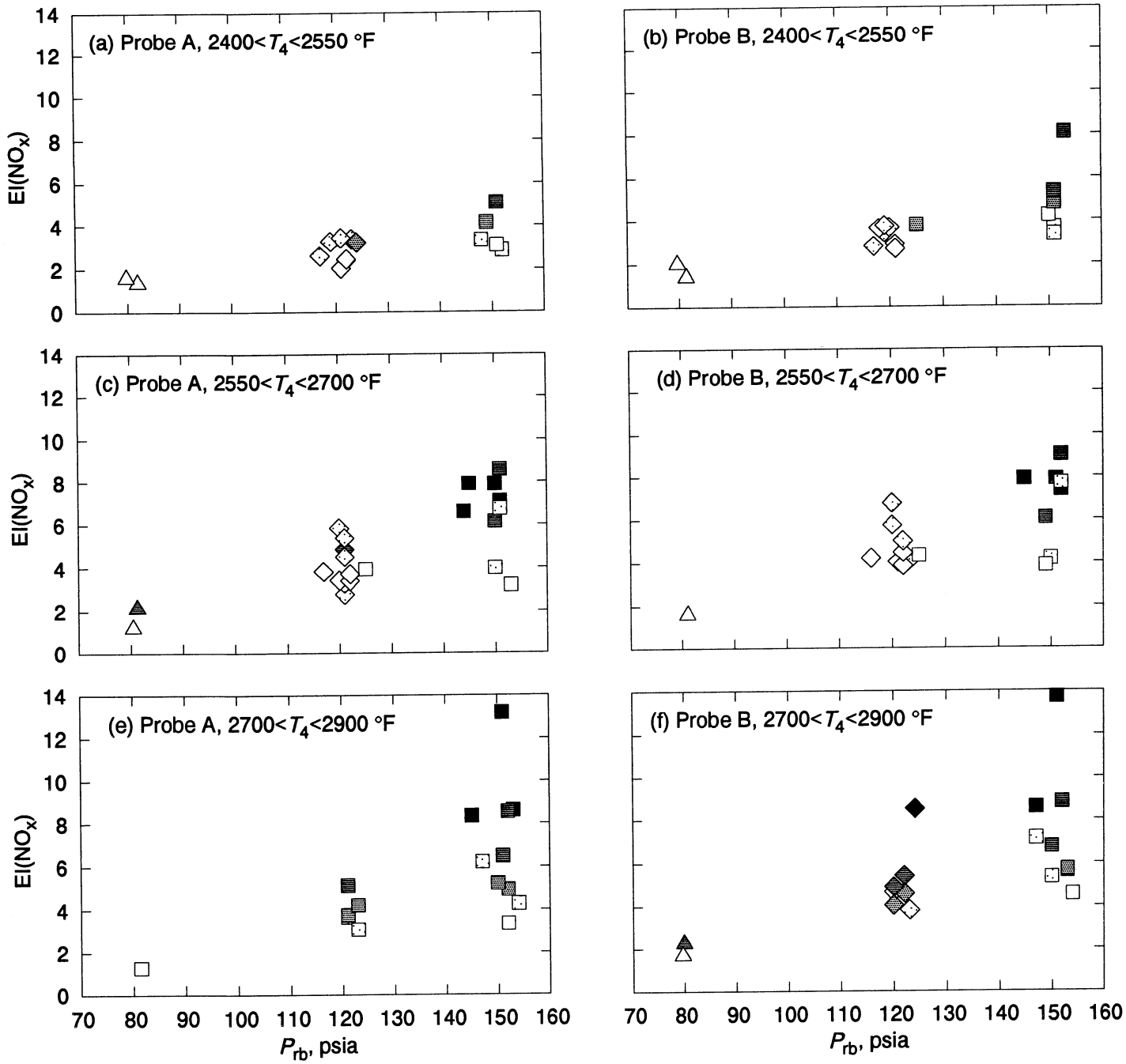

P_{rb} \ T_3	600	840	940	1000	1100
80	△	△	▲	▲	▲
120	◇	◇	◆	◆	◆
150	□	□	■	■	■

Figure 16. Variation of EI(NO_x) with combustor pressure.

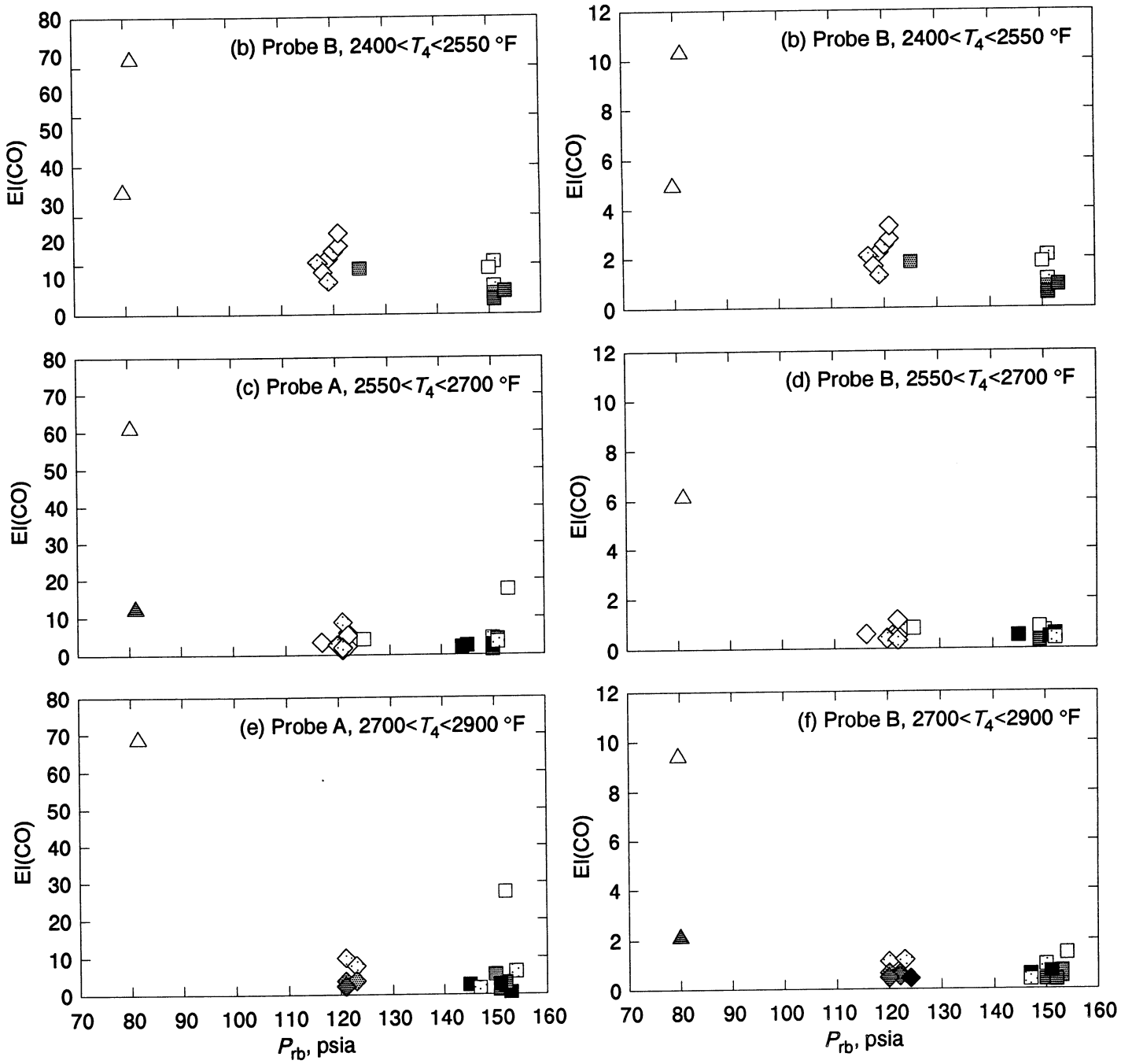

P_{rb} \ T_3	600	840	940	1000	1100
80	△	△	▲	▲	▲
120	◇	◇	◆	◆	◆
150	□	□	■	■	■

Figure 17. Variation of EI(CO) with combustor pressure.

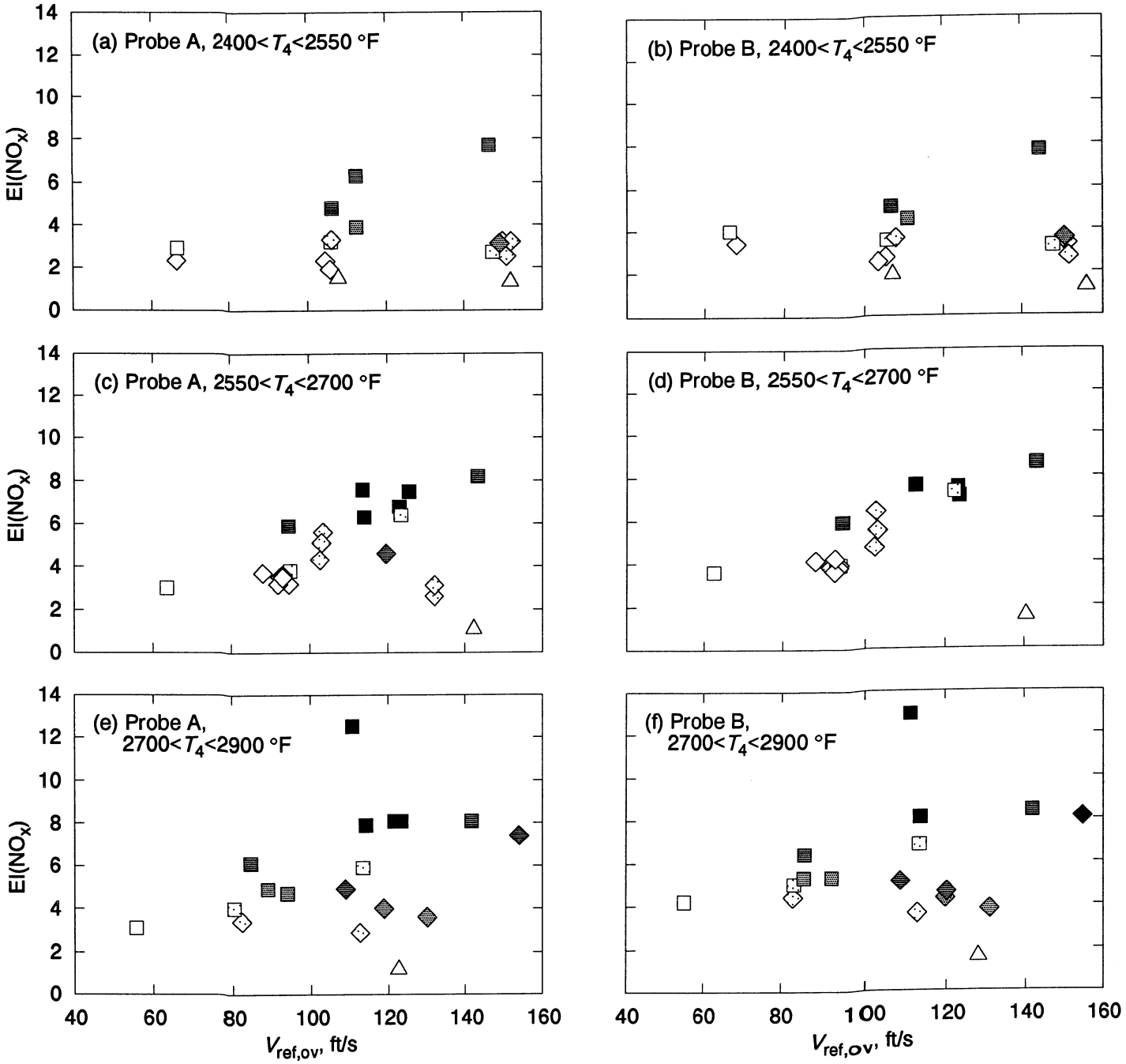

P_{rb} \ T_3	600	840	940	1000	1100
80	△	△	▲	▲	▲
120	◇	◇	◆	◆	◆
150	□	⊡	■	■	■

Figure 18. Variation of EI(NO_x) with $V_{ref,ov}$.

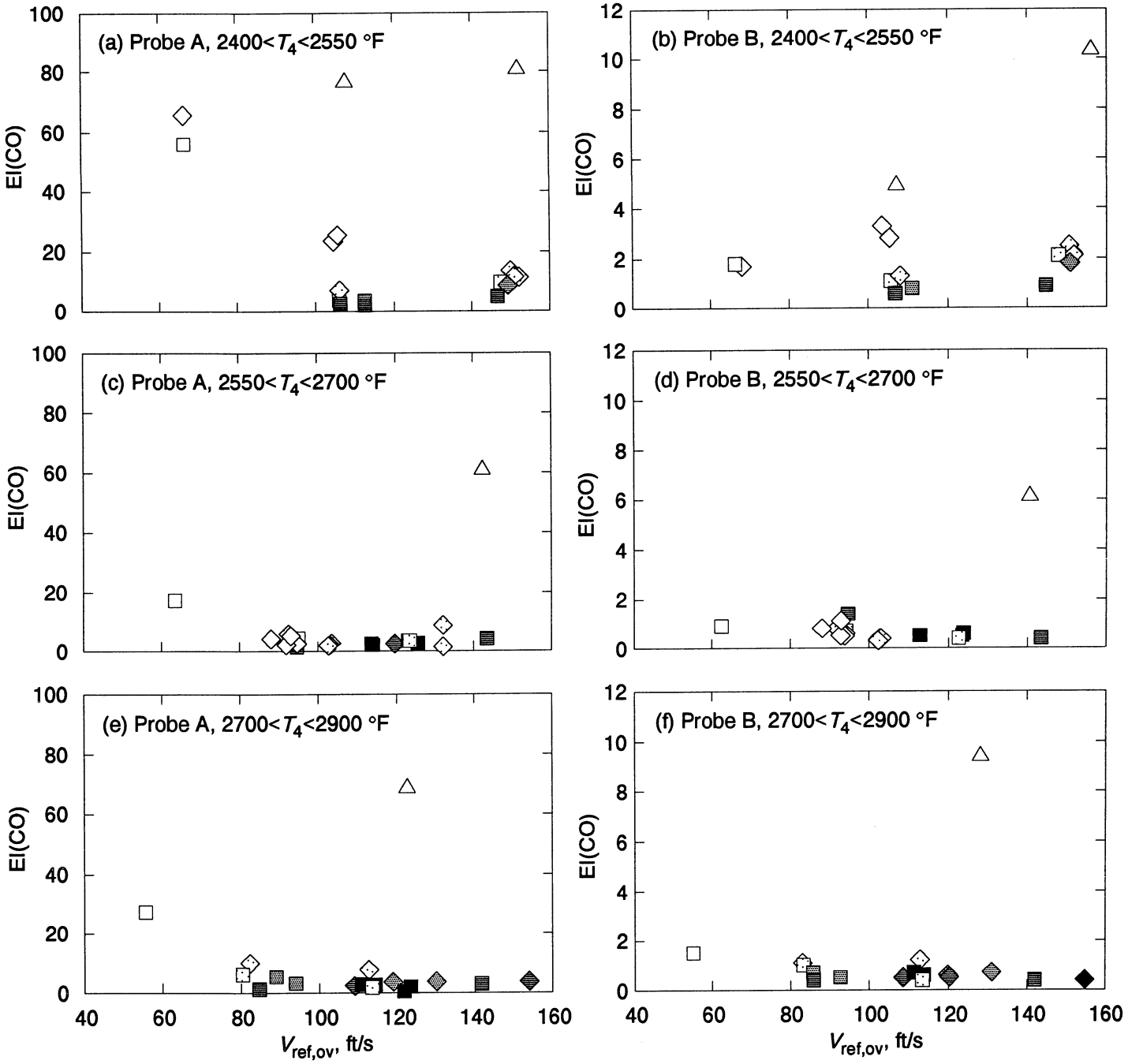

P_{rb} \ T_3	600	840	940	1000	1100
80	△	△	▲	▲	▲
120	◇	◇	◆	◆	◆
150	□	⊡	▩	▩	■

Figure 19. Variation of EI(CO) with $V_{ref,ov}$.

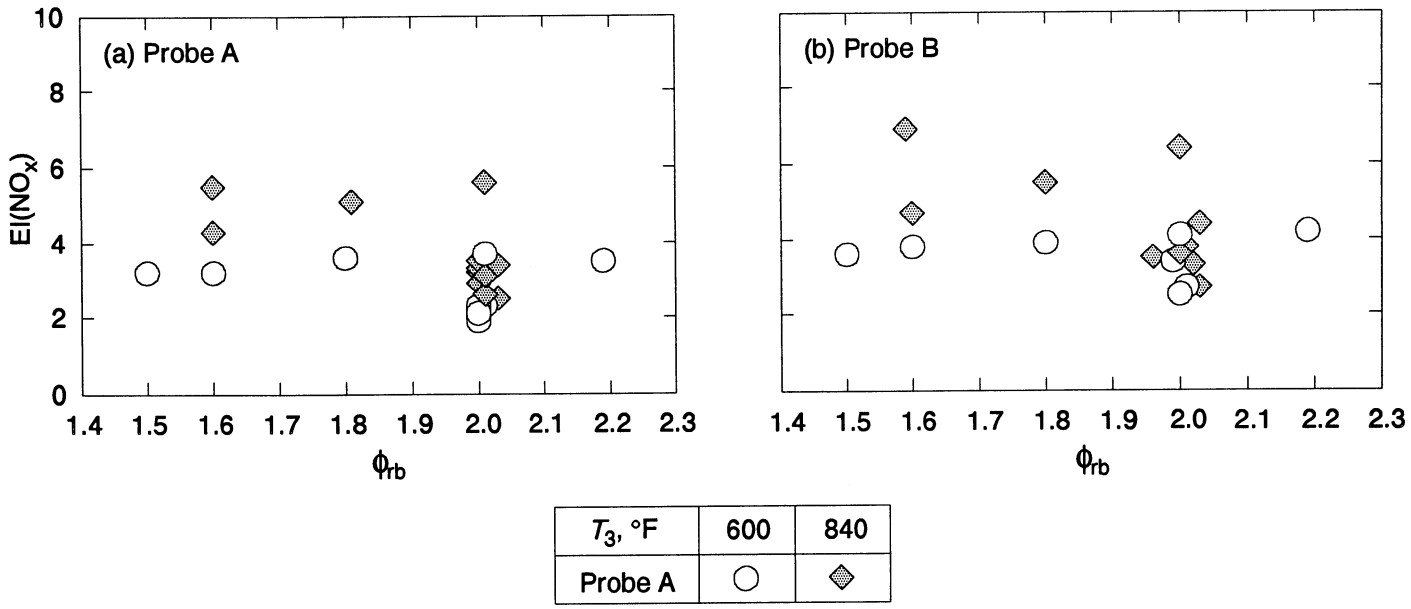

Figure 20. Variation of EI(NO_x) with rich-burn zone equivalence ratio.

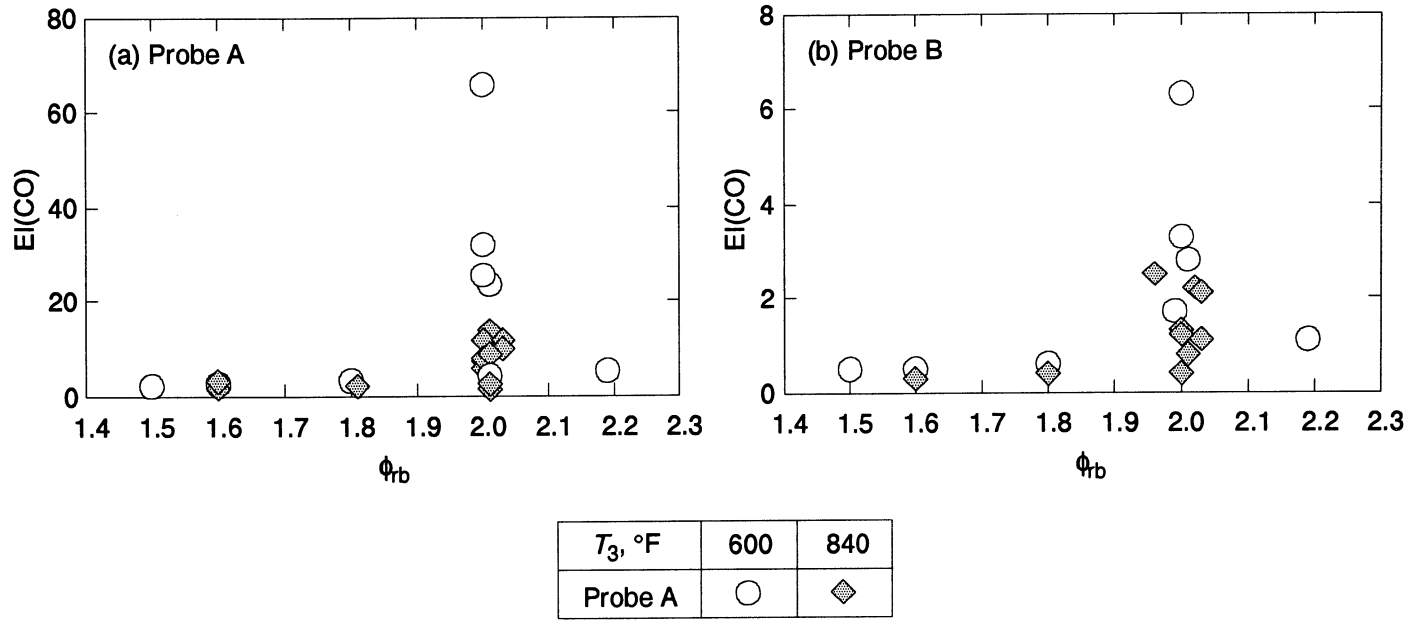

Figure 21. Variation of EI(CO) with rich-burn zone equivalence ratio.

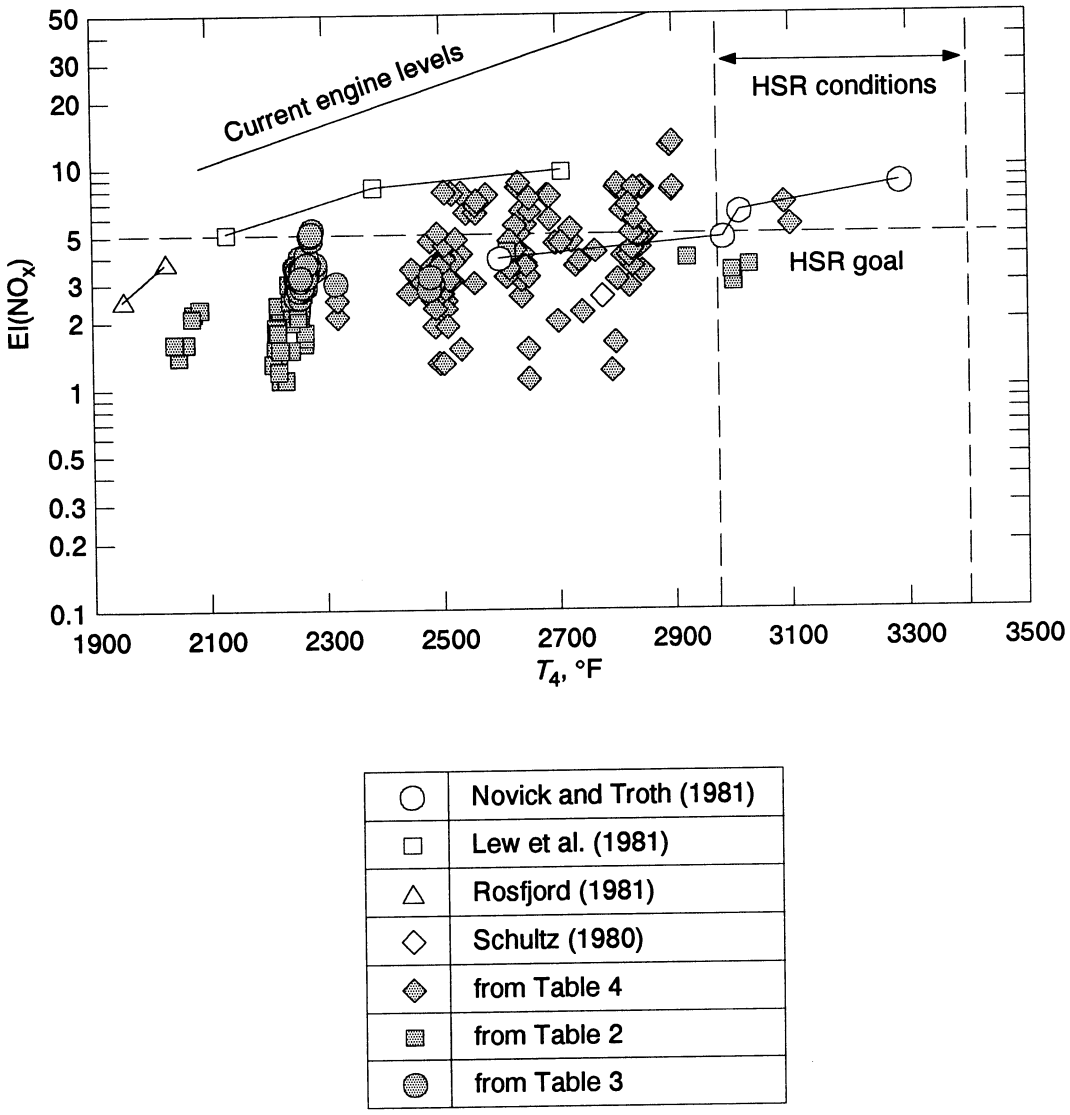

Figure 22. RQL combustor NO_x emission data at HSR conditions.

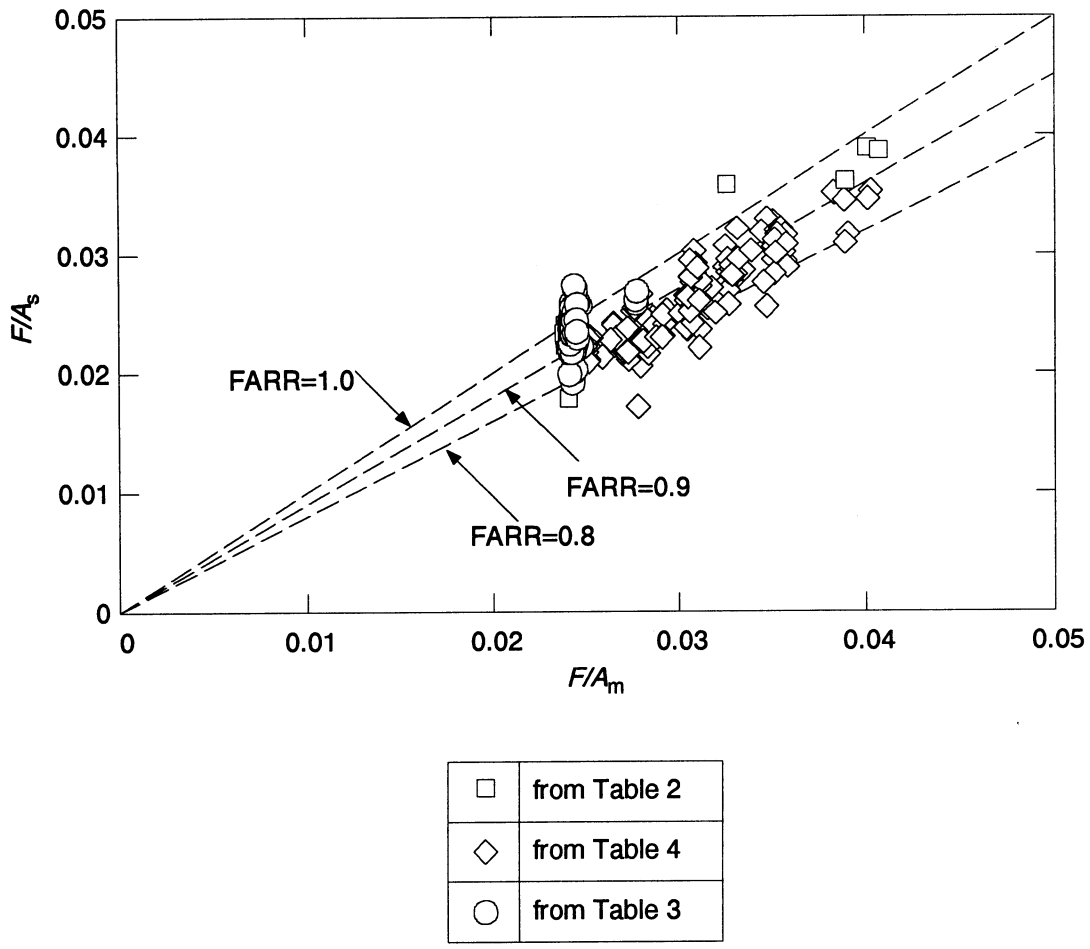

Figure 23. Gas-sampled fuel-to-air ratio versus metered fuel-to-air ratio for tests with Parker nozzle.

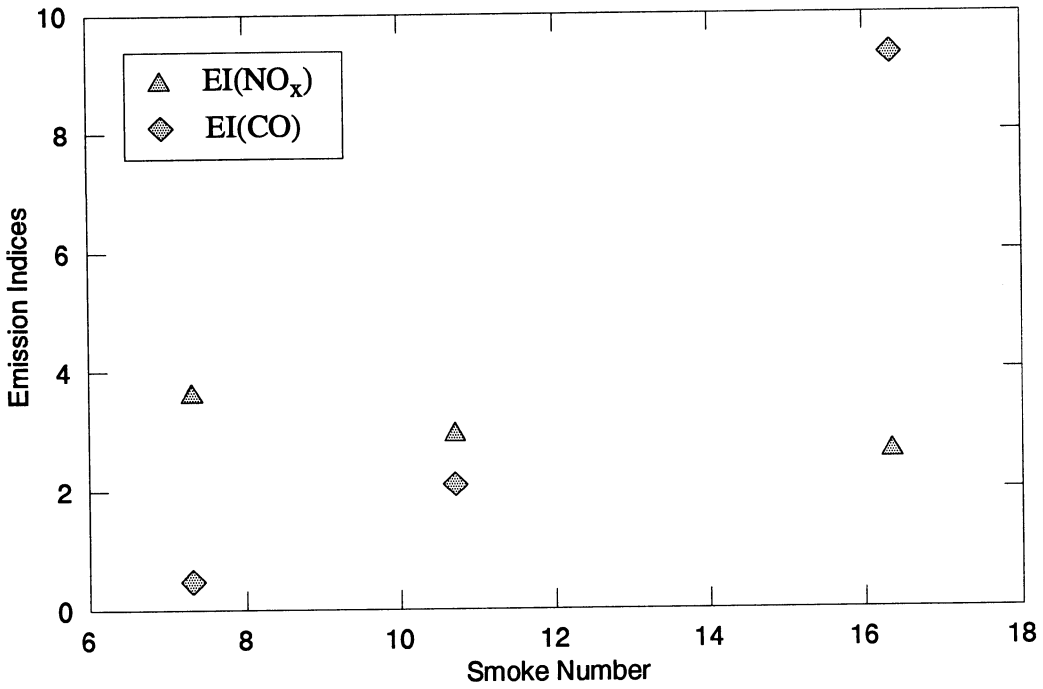

Figure 24. RQL combustor EI(NO_x) and EI(CO) versus smoke number. T_4=2500 °, T_3=840 °F, P_4=120 psia, ϕ_{rb}=2.0.

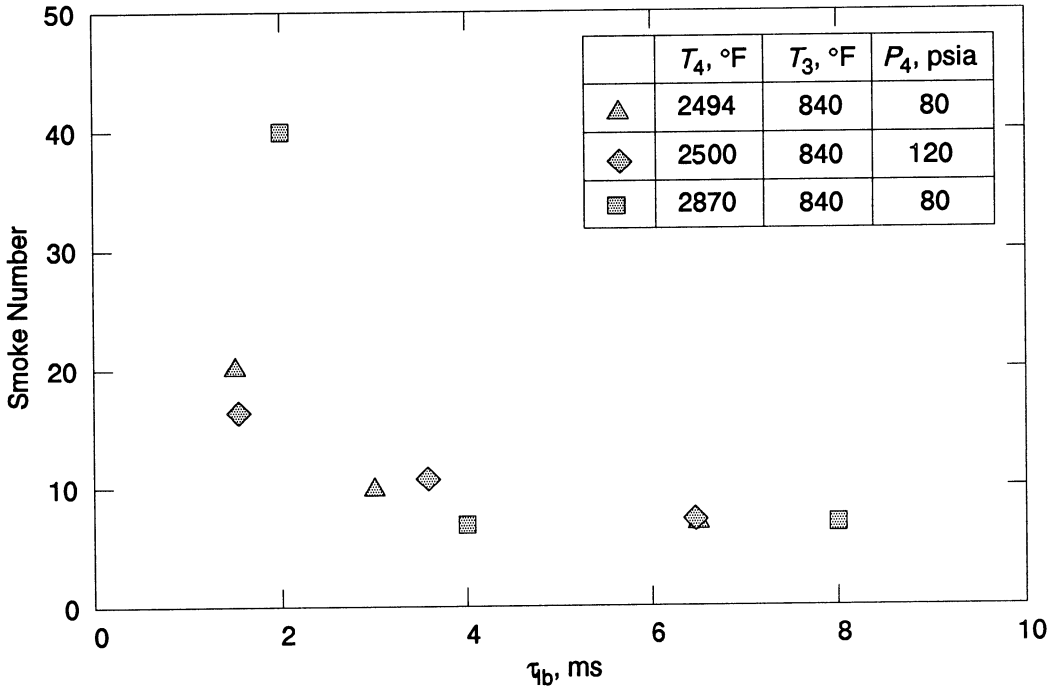

Figure 25. RQL combustor smoke number versus lean-burn residence time. ϕ_{rb}=2.0.

REPORT DOCUMENTATION PAGE

Form Approved
OMB No. 0704-0188

1. AGENCY USE ONLY (*Leave blank*)	2. REPORT DATE	3. REPORT TYPE AND DATES COVERED
	July 2001	Technical Memorandum

4. TITLE AND SUBTITLE

Low Emissions RQL Flametube Combustor Test Results

5. FUNDING NUMBERS

WU–714–01–40–00

6. AUTHOR(S)

Clarence T. Chang and James D. Holdeman

7. PERFORMING ORGANIZATION NAME(S) AND ADDRESS(ES)

National Aeronautics and Space Administration
John H. Glenn Research Center at Lewis Field
Cleveland, Ohio 44135–3191

8. PERFORMING ORGANIZATION REPORT NUMBER

E–12954

9. SPONSORING/MONITORING AGENCY NAME(S) AND ADDRESS(ES)

National Aeronautics and Space Administration
Washington, DC 20546–0001

10. SPONSORING/MONITORING AGENCY REPORT NUMBER

NASA TM—2001-211107

11. SUPPLEMENTARY NOTES

Responsible person, Clarence T. Chang, organization code 5830, 216–433–8561.

12a. DISTRIBUTION/AVAILABILITY STATEMENT

Document Availability Change Notice

This document was published in July 2001 with an EAR restriction. It was changed April 2003 to Unclassified/Unlimited per DAA modified February 11, 2003.

Export Administration Regulations (EAR) Notice

This document contains information within the purview of the Export Administration Regulations (EAR), 15 CFR 730–774, and is export controlled. It may not be transferred to foreign nationals in the U.S. or abroad without specific approval of a knowledgeable NASA export control official, and/or unless an export license/license exception is obtained/available from the Bureau of Industry and Security, United States Department of Commerce. Violations of these regulations are punishable by fine, imprisonment, or both.

Unclassified - Unlimited
Subject Category: 07 Distribution: Nonstandard

This publication is available from the NASA Center for AeroSpace Information, 301–621–0390.

12b. DISTRIBUTION CODE

13. ABSTRACT ***(Maximum 200 words)***

The overall objective of this test program was to demonstrate and evaluate the capability of the Rich-burn/Quick-mix/Lean-burn (RQL) combustor concept for HSR applications. This test program was in support of the Pratt & Whitney and GE Aircraft Engines HSR low-NO_x Combustor Program. Collaborative programs with Parker Hannifin Corporation and Textron Fuel Systems resulted in the development and testing of the high-flow low-NO_x rich-burn zone fuel-to-air ratio research fuel nozzles used in this test program. Based on the results obtained in this test program, several conclusions can be made: (1) The RQL tests gave low NO_x and CO emissions results at conditions corresponding to HSR cruise. (2) The Textron fuel nozzle design with optimal multiple partitioning of fuel and air circuits shows potential of providing an acceptable uniform local fuel-rich region in the rich burner. (3) For the parameters studied in this test series, the tests have shown T_3 is the dominant factor in the NO_x formation for RQL combustors. As T_3 increases from 600 to 1100 °F, EI(NO_x) increases approximately three fold. (4) Factors which appear to have secondary influence on NO_x formation are P_4, T_4, ϕ_{rb}, $V_{ref,ov}$. (5) Low smoke numbers were measured for ϕ_{rb} of 2.0 at P_4 of 120 psia.

14. SUBJECT TERMS	15. NUMBER OF PAGES
RQL combustor; Emissions; Gas turbine combustor	50
	16. PRICE CODE

17. SECURITY CLASSIFICATION OF REPORT	18. SECURITY CLASSIFICATION OF THIS PAGE	19. SECURITY CLASSIFICATION OF ABSTRACT	20. LIMITATION OF ABSTRACT
Unclassified	Unclassified	Unclassified	